LBL-33082
UC-331

Lawrence Berkeley Laboratory
UNIVERSITY OF CALIFORNIA

ENERGY & ENVIRONMENT
DIVISION

Performance of Sodium/Phosphorus-Sulfur Cells and Phase Equilibria of Sodium-Phosphorus-Sulfur Mixtures

P.L. Ridgway*, F.R. McLarnon, and E.J. Cairns
*(M.S Thesis)

September 1992

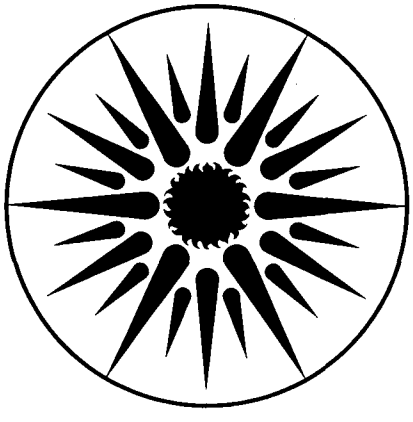

ENERGY & ENVIRONMENT
DIVISION

Prepared for the U.S. Department of Energy under Contract Number DE-AC03-76SF00098

DISCLAIMER

LBL-33082

PERFORMANCE OF SODIUM/PHOSPHORUS-SULFUR CELLS AND PHASE EQUILIBRIA OF SODIUM-PHOSPHORUS-SULFUR MIXTURES

by

Paul L. Ridgway, Frank R. McLarnon and Elton J. Cairns

Energy & Environment Division
Lawrence Berkeley Laboratory
University of California
Berkeley, California 94720

This work was supported by the Assistant Secretary for Conservation and Renewable Energy, Office of Transportation Technologies, Electric and Hybrid Propulsion Division of the U.S. Department of Energy under Contract No. DE-AC03-76SF00098.

Table of Contents

Figures

Tables

Introduction

The importance of electrical energy to modern society cannot be overstated. The ability to store electricity in portable containers, commonly called "batteries", is an essential aspect of the usefulness of this form of energy. Batteries are ubiquitous in the civilized world, and significant improvements in them are certain to benefit all of us.

Batteries are groups of interconnected electrochemical "cells" which individually harness the energy released by a spontaneous electrochemical reaction. Electrochemical reactions are those wherein electrons are transferred from one atom or molecule of reactant to another during formation of the reaction product(s). If the reactants are physically mixed, the physical contact of reactants, electron-transfer and formation of products occur in the same location, and the energy of the reaction produces heat (and perhaps electromagnetic radiation).

In an electrochemical cell, the electron transfer is separated from the rest of the reaction process. The electrons, as electrical current, are passed from one of the reactants through an external circuit to the other reactant in the cell. The electricity in the external circuit can be made to do work such as operate a motor, produce light, etc.

The cell operates by separating the reactants physically and electrically, but connecting them ionically, by way of the "electrolyte". The electrolyte is a physical barrier and an electronic insulator, but is ionically conductive. The chemical reactants in the cell (called electrodes) as well as the electrolyte can be either liquid or solid. When the electrodes are electrically connected by way of the external circuit, electrons pass through the circuit, forming electrically charged reaction intermediates (ions) in both electrodes. Depending on the nature of the cell and the chemical reaction involved, the ions from one or the other or both electrodes pass into the electrolyte. The ions combine to form the reaction product in the electrolyte or at one of the electrodes. If the cell is rechargeable, the process can be reversed by connecting it to an external electrical power source.

Any spontaneous electrochemical reaction could be used in a cell to generate electricity. In choosing reactions which will be most useful, one obvious factor considered is the energy of the reaction per unit weight of the cell, or the specific energy of the cell. Another is the reaction rate, which limits the current output, or power output from the cell. The higher the specific energy and power the better the cell.

A 'theoretical specific energy' of the cell can be calculated by dividing the Gibbs free energy of a reaction by the weight of the reactants. This gives a theoretical maximum value for the specific energy of the cell because it assumes that the weight of the cell parts is insignificant compared to the weight of the reactants. This calculation is useful in comparing candidate reactions for use in energy storage cells.

The highest energy reactions which have been found suitable for secondary (rechargeable) storage batteries require high temperatures because of the very low reaction rates at room temperature or low conductivity of the compatible electrolyte. All of the electrochemical reactions represented in Figure 1[1] with a theoretical specific energy of over 800 watt-hr/kg operate above room temperature, except Zn/MnO_2 which has not yet been made into a practical secondary cell. The sodium/sulfur cell for example must operate over 285 °C to keep the reaction product, which forms in the sulfur electrode, from forming a solid precipitate within the molten sulfur electrode, inhibiting further reaction.

Project Motivation

The hypothesis that forms the basis of this work is that the addition of phosphorus to the sulfur electrode may improve the performance of the sodium/sulfur cell. However, new informa-

tion has also been gained on the phase equilibria of sodium-phosphorus-sulfur mixtures. Apparently very little has been published on this subject.

The sodium/sulfur cell has been the subject of research and development for at least 26 years[2]. It consists of molten sodium and molten sulfur electrodes separated by a solid sodium ion conducting electrolyte, and is typically operated near 350°C. Upon discharge sodium cations pass through the electrolyte into the sulfur electrode and combine with anionic polysulfide chains of varying length to form sodium polysulfides, the reaction product[3]. Factors which affect the performance of the sulfur electrode include conductivity as influenced by viscosity and ionic strength, the energy of the reaction with sodium, the number of liquid phases (one or two) present, and the effective equivalent weight of the sodium-sulfur combination.

In this chapter we consider the characteristics of the sulfur electrode, the properties of phosphorus sulfides, and previous work with lithium/phosphorus-sulfur cells that give reason to expect that sulfur electrode performance in a sodium/sulfur cell might be improved by the addition of phosphorus. Also in this chapter we discuss the experimental method, and explain the interpretation of data with respect to the phase equilibria of the Na-P-S ternary system.

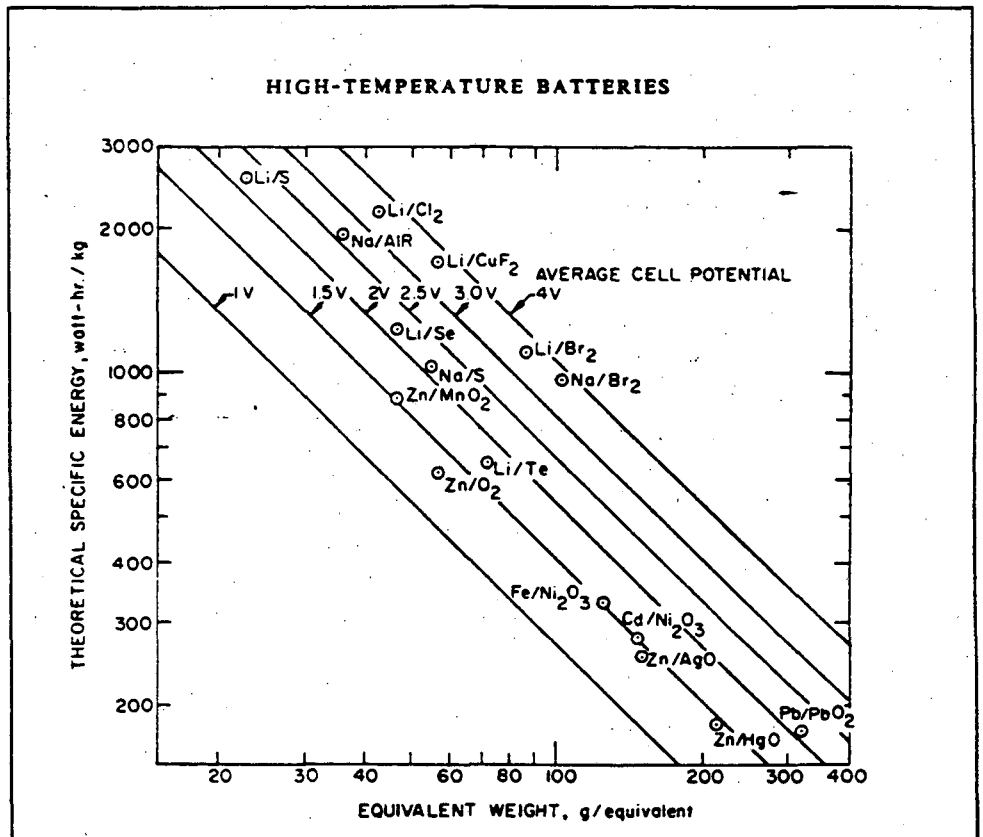

Figure 1. A selection of high energy electrochemical reactions for energy storage[1].

Conductivity

As positive electrode materials, both pure sulfur and phosphorus-sulfur mixtures have the disadvantage of being poor electronic and ionic conductors. During cell discharge, the highly mobile sodium ions entering the positive electrode melt function as an electrolyte within the melt, giving ever-increasing ionic conductivity to it, decreasing overall cell resistance, thereby improving cell performance[4].

When the cell is charged, the process is reversed. The sodium passes back out of the positive electrode at the electrolyte interface, eventually creating a highly resistive, sodium-poor layer there. This makes the charging process slow and energy-inefficient. It is during the charging of a nearly fully charged cell that the sulfur electrode's performance degrades rapidly and where modifications to increase conductivity will have the greatest effect.

The sodium-sulfur binary phase diagram (Figure 2)[5] shows the cause of this problem. At temperatures above 240°C mixtures of sodium and sulfur of composition ranging from 79 to nearly 100 wt % sulfur split into two liquid phases. One is relatively sodium-rich, ionically conductive, and inviscid (27 atom % Na, conductivity 0.39 $\Omega^{-1}cm^{-1}$ viscosity 18.6 cP at 350°C) and the other is sodium poor, six orders of magnitude more resistive, and highly viscous (0.013 atom % Na, conductivity $10^{-8}\Omega^{-1}cm^{-1}$, pure sulfur viscosity 500 Cp at 350°C).[6,7]

The tendency during charge to create the highly resistive layer is countered by the diffusion of sodium from the bulk melt to the electrolyte surface. Diffusion is relatively rapid as long as the bulk sodium content is above 21 wt % (27 atom %) because the driving force is high and the viscosity is low in the one equilibrium phase that exists.

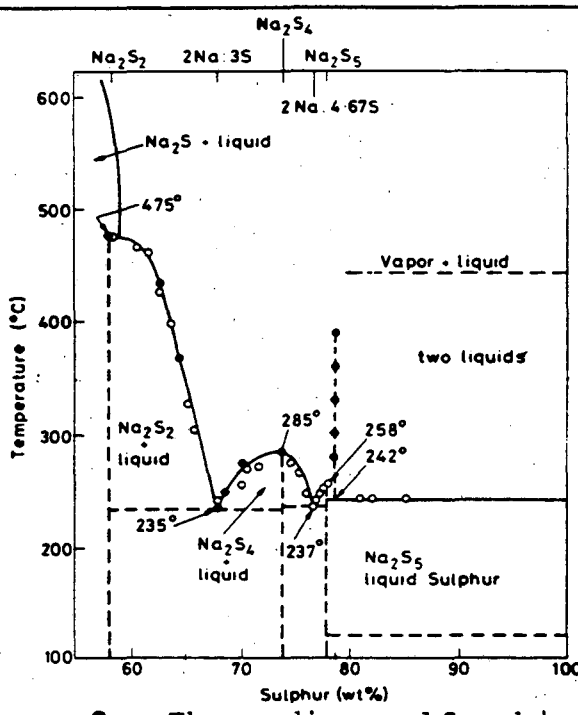

Figure 2. The sodium-sulfur binary phase diagram[7].

When the overall composition the sulfur electrode drops below 21 wt % Na, the highly resistive sodium-poor phase described above coats the electrolyte stably, i.e. no matter how slowly the cell is charged (or even under no current) the resistive coating does not dissipate, because it is at equilibrium with the phase 20 times more concentrated in sodium.

Other workers have introduced additives to the sulfur melt which have improved conductivity in the electrode via viscosity reduction (1 mole % selenium) or by a combination of viscosity reduction and increase in conductivity via generation of charged species (@ 1 mole % tetracyanoethylene). They

reported a doubling of charge acceptance at given current densities.[8]

Phosphorus may aid sulfur electrode performance by both viscosity reduction and an increase in concentration of charge carriers. The phosphorus pentasulfide-sodium sulfide phase diagram (Figure 3)[9] shows that a phosphorus sulfide electrode would have a two-phase region similar to that of a sulfur electrode, except that the sodium-poor phase would have about 500 times more sodium in it. Also, the phosphorus pentasulfide viscosity is about 1.5 Cp, or 1/300 that of sulfur at 350°C[10]. An increase in ionic strength and decrease in viscosity in the inevitable sodium-poor phase can be expected to increase the charging current dramatically, at least in the final stages of charge, as shown in the literature cited above.

On the other hand, phosphorus is known to form viscous, glassy systems in combination with sodium and sulfur. Mixtures of P_2S_5 with 0 - 66 mole % Na_2S form glasses[11]. A highly viscous positive electrode melt is disadvantageous to the power output of this cell as it slows diffusion of reaction products from the electrolyte interface into the bulk electrode.

This does not prohibit the possibility that P/S ratios considerably below that of P_2S_5 may perform significantly

better than a pure sulfur electrode. In addition, previous work with Li/P_2S_5 cells gave promising results, as discussed below. The elements Li and Na have very similar chemical properties, and it is likely that the effect of phosphorus in systems containing Na or Li will be similar.

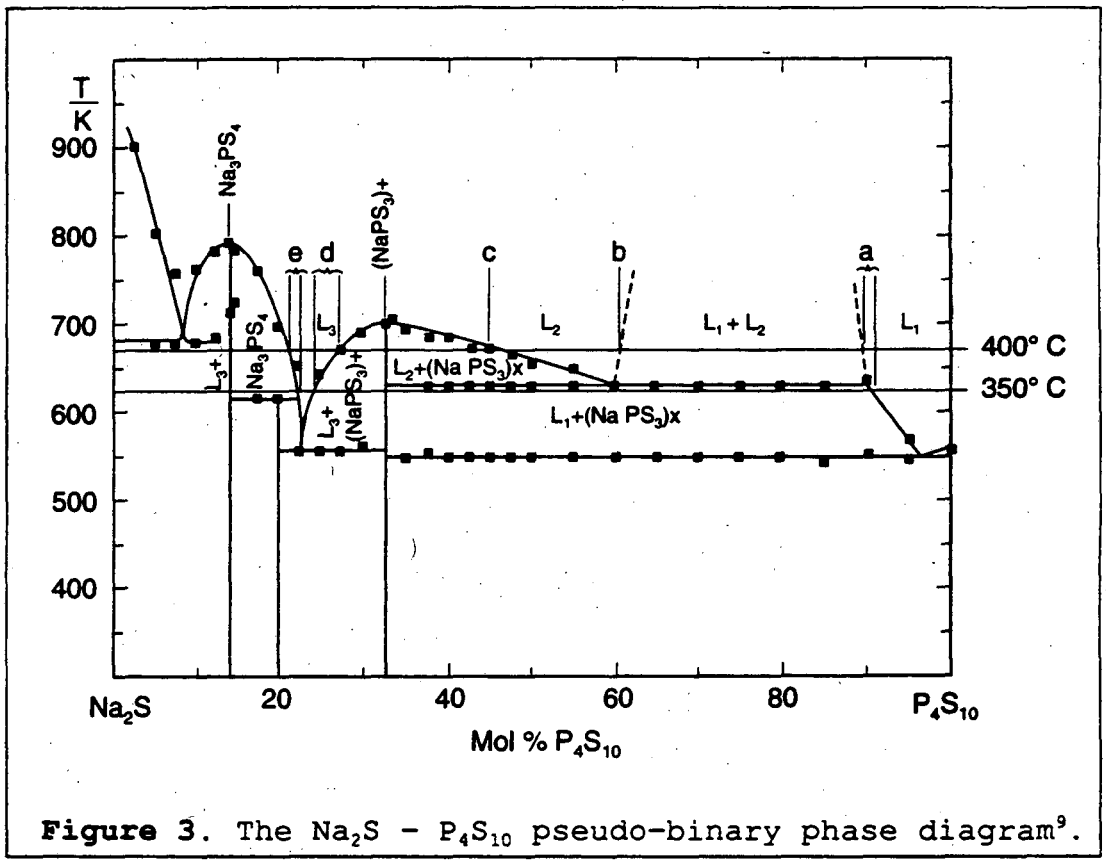

Figure 3. The Na_2S - P_4S_{10} pseudo-binary phase diagram[9].

Equivalent Weight

The ultimate product of the reaction of sodium with phosphorus is Na_3P and with sulfur it is Na_2S. Thus the molar amount of phosphorus required to react with a given amount of sodium could be less than the equivalent amount of sulfur. Specific

energy is a strong function of equivalent weight, as shown in Figure 1. Thus a cell containing some phosphorus may have a greater specific energy than the standard sodium/sulfur cell.

Temperature

The sulfur electrode and its variants are only useful if completely molten because the cell reaction products must be able to diffuse away from the melt/electrolyte interface into the bulk electrode melt. The formation of solids inhibits this process and may prevent full use of the energy content of the cell. Thus the cell temperature must be high enough to keep the electrode completely liquid.

Unfortunately, a sodium-phosphorus-sulfur mixture is likely to be higher melting than the corresponding sodium-sulfur mixture. For example Figure 3 shows that a solid with a melting point of about 430°C forms at a composition of 33 mole % P_4S_{10} (atom-fractions $\chi_P, \chi_S, \chi_{Na}$ = 0.20, 0.60, 0.20). Thus an electrode with a P/S atom-ratio of 0.3 would have to be operated at temperatures above 430°C to achieve a depth of discharge comparable to that of the sulfur electrode, which is routinely discharged to χ_{Na} = 0.4 at 350°C.

Previous Studies of the Phosphorus-Sulfur Electrode

The performance of lithium/molten salt/sulfur and lithium/molten salt/phosphorus-sulfur cells have been compared in the literature. One report gave extrapolated data indicating that the lithium/phosphorus-sulfur cell may give higher capacity densities (amp-hr/electrode area) than the lithium/sulfur cell, at high current densities (>1 A/cm^2)[12]. A later report showed significantly higher open circuit voltages in the lithium/P_2S_5 cell (2.7 vs. 2.3 volts)[13]. Higher cell voltages during discharge combined with a lower equivalent weight for phosphorus would suggest a higher specific energy cell. This report claims to have discharged lithium/phosphorus-sulfur cells at rates as high as that for lithium/sulfur cells, and to have obtained slightly higher cell voltages, and asserts that slightly higher specific energies (than for Li/S cells) might be possible. It is plausible that phosphorus would have a similar effect in the sodium/sulfur cell.

Equilibrium EMF Measurements

The principal experiment in this project was the gathering of open circuit potential measurements for sodium/phosphorus-sulfur cells at various states of charge, temperatures, and P/S ratios. The data obtained is thermodynamic in character, and does not include the kinetic information obtained in cell

performance testing as reported in the previous work[13] on lithium/phosphorus-sulfur cells. It is a useful screening method, however, for determining temperatures and phosphorus/sulfur ratios which may give high performance.

Equilibrium EMF Data as an Indicator of Cell Performance

Integration of plots of equilibrium cell voltage versus coulombs passed gives the theoretical maximum energy which could be obtained from the cell if it was discharged "reversibly" (infinitely slowly). The theoretical maximum specific energy available via the discharge of a cell can be calculated via the expression

$$Sp.E. = \frac{\int_0^{\alpha} \varepsilon(c)\, dc}{m_{Na} + m_{PS}}$$

where α is the number of coulombs of charge **c** required to discharge a fully charged cell to a positive electrode composition of $\chi_{Na} = 0.4$, which is the typical discharge limit of the Na/S cell; m_{Na} is the mass of the sodium consumed in the passage of α coulombs; m_{PS} is the mass of all of the phosphorus and sulfur in the positive electrode; and $\varepsilon(c)$ is the cell emf. The integral is evaluated graphically. The

result of this calculation from the sodium/sulfur cell data is compared to that from cells with phosphorus-sulfur electrodes.

EMF Studies as a Probe of Liquid-Phase Equilibria

Equilibrium EMF data can also be used to gain information about the areas of the ternary Na-P-S phase diagram traversed during the operation of the cell. The equilibrium, open-circuit potentials of the sodium/phosphorus-sulfur cell are a direct measure of the chemical potential of sodium in the phosphorus-sulfur electrode versus pure molten sodium at the same temperature. This is expressed by the Nernst equation:

$$E=E_o-\frac{RT}{nF}\ln\frac{\alpha_{Na^*}}{\alpha_{Na}}$$

In the cells used in this work, the sodium activity α_{Na} in the sodium electrode is always 1. The standard potential E_o equals the cell potential E when the logarithmic term is zero: This corresponds to the hypothetical case where the sodium activity in the P-S electrode α_{Na^*} is 1, or in other words, when a pure molten sodium phase exists at equilibrium in the P-S electrode. Also in this case, since the sodium activity in both electrodes is 1, the sodium chemical potential in both electrodes is equal, and the cell electrical potential E is zero. Thus E_o is shown to be zero for our cell and can be dropped from the above equation. Introducing these restric-

tions and rewriting the sodium activity as the product of its mole fraction χ_{Na^*} times its activity coefficient γ_{Na^*} the equation becomes

$$E=-\frac{RT}{nF}\ln\gamma_{Na^*}\cdot\chi_{Na^*}$$

Thus, as more sodium is added, the cell potential E decreases linearly in a plot versus the logarithm of sodium concentration if, as is observed for the sulfur electrode at low sodium concentrations, γ_{Na^*} is approximately constant.

However, activity coefficients change abruptly when a changing electrode composition results in transition from one phase field to another. This is what allows cell emf measurements to elucidate phase equilibria. For example, as the cell is discharged, the increasing concentration of sodium in the positive electrode melt can cause a single liquid phase to split into two liquid phases.

By the Gibbs phase rule for this (or any) <u>three</u> component system, a maximum of three phases can coexist at equilibrium. While three phases exist at equilibrium, in any proportion, their compositions will remain fixed, though the relative amounts of each phase can change.

While discharging or charging a cell through a three phase region, the relative amounts of each of the three phases

change in response to the change in the overall amount of sodium in the electrode. For example, on discharge through a three-phase region, the overall concentration of sodium in the P-S electrode will increase. This will cause an increase in the amount of the sodium-rich phases, and a decrease in the amount of the phase containing the least sodium. However, the chemical compositions of the phases remain constant, and so the sodium chemical potential remains constant. Thus, throughout a three phase region of the Na-P-S system the electrode potential is constant; The slope of a plot of E vs χ_{Na} is zero for a cell discharge through such a region.

Usually, a transition between single-phase and two-phase regions will cause an abrupt change in the slope of E vs χ_{Na}. Compared to a single-phase region, the opportunity in a two-phase region to partition a change in overall sodium content between those two phases to obtain a free energy minimum will most likely cause a decrease in the slope of the equilibrium discharge curve.

On the other hand, a change in slope can occur due to a change in electrode reaction, such as the number of electrons transferred per "mole of reaction" (the constant **n** in the Nernst equation). This could be misinterpreted as a passage through a phase boundary. Confirmation of a phase change can be obtained by looking at the slope of potential vs tempera-

ture at the state of discharge where the previously described slope change was observed. As long as the overall composition at the phase boundary varies with temperature, the slope of EMF vs Temp will have a break at the temperature at which the break in slope of EMF vs χ_{Na} was observed previously. If there had been no phase boundary, no break in slope would be observed.

Usually phase equilibria of high-temperature systems are studied by differential thermal techniques as well, so this work is incomplete in this respect. However, the primary purpose of this work is to determine the utility of this system for electrical energy storage. Thus this electrochemical technique is appropriate to our intent. Since the resulting data provide information on the phase equilibria as well, the data are used to construct phase diagrams of the Na-P-S system as well.

The constant n in the Nernst equation can be determined from equilibrium cell emf data for the cell reaction when the following assumptions are valid: 1) There is only one reaction product. 2) The product's activity coefficient is constant (possible if the data collected to calculate n cover a very small range in concentration of the product - Henry's law if the concentration is very low. 3) The activities of the reactants are constant: The reactants are pure sodium (in the

sodium electrode at a constant activity of 1), and the cathode melt. The activities of the components of this melt are roughly constant over the very slight change in solute concentration postulated in assumption 2).

From assumption 1) we can write a semi-generic cell reaction:

$$xNa + C \rightarrow Na_xC$$

where C is the reactant in the cathode melt. The corresponding Nernst equation is:

$$E=E_0-(\frac{RT}{nF})\ln(\frac{\alpha_{Na_xC}}{\alpha^x_{Na^0_{liq}}\alpha_C})$$

Since there is only one reaction product, the equation can be rearranged as

$$E=E_0+(\frac{RT}{nF})\left[\ln(\frac{\alpha^x_{Na^0_{liq}}\alpha_C\chi}{\gamma_{Na_xC}})\right]-(\frac{RT}{nF})\ln\chi_{Na}$$

If, for the reasons discussed above, the activity of sodium in the sodium electrode, the activity of the reactant CR in the positive electrode, and the activity coefficient of the product are constant with respect to χ_{Na}, the first two terms in the above equation are constant with respect to χ_{Na}. Thus,

$$\frac{dE}{d\ln(\chi_{Na})} = -\frac{RT}{nF}$$

from which it can be seen that **n** can (in principle) be obtained from the slope of a plot of cell emf versus $\ln\chi_{Na}$. This was attempted as discussed in the results section of this thesis.

Experimental Apparatus and Procedures

The experimental work required considerable effort to create a system which could provide the desired data. The combination of high temperatures and reactive chemicals required the use of specialized materials in apparatus design in an inert atmosphere. The slow accumulation of data necessitated continuous automated control and data collection.

Materials and Apparatus

Glove Box

A helium-atmosphere glove box equipped with oxygen and moisture removal housed the experiments[14] . Oxygen and water concentrations were less than 1 and 5 ppmv respectively as measured by a trace oxygen analyzer and a hygrometer[15]. A cylindrical furnace-well, 12.7 cm in diameter and 67.3 cm deep, set in the floor of the glove box, allowed heating of the electrochemical cell.

Chemicals

The chemicals used in this work were sodium metal[16], sulfur[17], sodium sulfide (Na_2S)[18], sodium phosphide (Na_3P)[19],

phosphorus pentasulfide (P_4S_{10})[20], tetraphosphorus trisulfide (P_4S_3)[21], and graphitized carbon black[22].

The sulfur and P_4S_{10} had sharp melting points and were used without further purification, as were the Na_2S and Na_3P. For EMF studies, the sodium was further purified immediately before charging the cell by a procedure described below. The P_4S_3 was sublimed twice, after which the melting range was 171-174°C.

EMF Cell

The creation of a practical experimental cell for the emf studies was by far the most challenging part of the project, mostly due to the lack of available expertise in the design and construction of such a high-temperature pressure vessel with essentially leak-free demountable seals.

The emf cell consists of a positive electrode compartment containing a molten phosphorus-sulfur mixture, and a negative electrode compartment containing molten sodium. These compartments are separated and electrically insulated from each other by a solid electrolyte which allows sodium ions to pass back and forth between the compartments.

This electrolyte is a modified alumina ceramic manufactured as a fine-grained mixture of two crystalline phases called β and β″-alumina. In our case it is sintered into a nonporous, closed-end tube with an ionic resistivity of 3-5 Ω-cm at 300°C[23]. It has the approximate composition of $Na_2O \cdot 11Al_2O_3$ plus 1 to 2 wt % Li_2O or MgO to stabilize the formation of the more conductive β″ phase[24]. It has been studied for many years and many references are available on the subject[25].

A cross sectional view of the cell in Figure 4 shows three main parts. The cell bottom is a closed-end Type 304 stainless steel tube welded to a Type A286 steel flange. The electrolyte assembly is an α-alumina collar (the "header") sealed to a β″-alumina closed-end tube. The header was bonded to the electrolyte tube using a proprietary sealing glass[26].

The cell top is a comparatively complex construction of steel and molybdenum. Molybdenum was used for corrosion resistance where there is contact with phosphorus and sulfur liquid or vapor, and A286 steel gives the flange torsional strength. The molybdenum part of the cell top includes the current collector (a closed end tube which also serves as a thermocouple well), a valve (which allows evacuation of the positive electrode vapor space after assembly), and forms the critical "sealing disk" which is pressed against the electrolyte header to form the sealing joint.

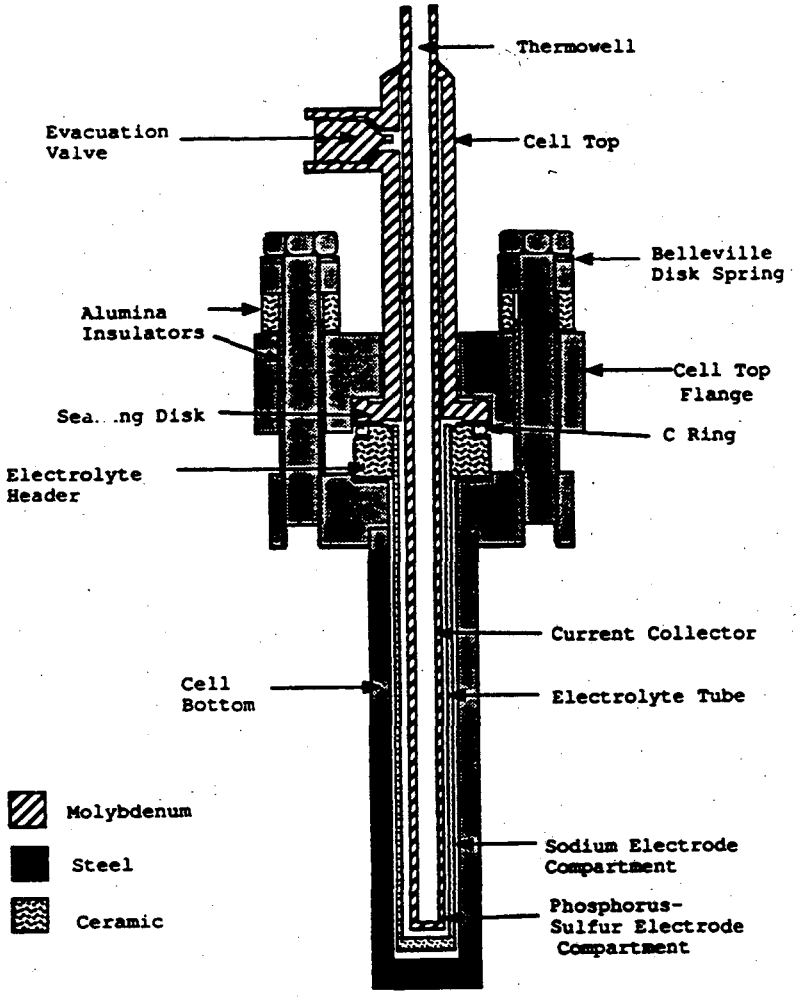

Figure 4. Diagram of the EMF cell.

At the high operating temperatures anticipated, a gas-tight seal of the P-S electrode compartment was required. At the design-limit temperature of 500°C, pure sulfur has an absolute vapor pressure of about 200 kPa, and sodium about 0.7 kPa. The loss of a small amount of the sodium electrode due to vaporization would not affect our measurements, so a hermetic

seal of this electrode compartment was not attempted. The phosphorus-sulfur compartment requires a very good seal because of the relatively high vapor pressure of the very small amount (@ 1/2 gram) of material used. Vapor loss here would directly affect the composition of the positive electrode, and thereby, the cell potential.

A workable solution to the surprisingly difficult problem of obtaining a leak-free seal under these conditions involved several design elements. A commercially available high-temperature spring-gasket called a "C-ring"[27] was used in conjunction with high-temperature disk-springs[28] to counter loosening of the seal-joint due to thermal expansion. As the C-ring is a hard material (inconel alloy) a soft gasket material was used between the C-ring and the electrolyte header and between the C-ring and the cell top. Aluminum foil[29] gaskets were used both above and below the C-ring. The gaskets were spray-coated with graphite[30], which allowed easier disassembly of the cell after use but did not decrease sealing power, as determined by helium leak tests up to 500°C. Figure 5 and Figure 6 are photographs of the disassembled and the assembled cell, respectively.

On cell assembly, the current collector of the cell top fits into the electrolyte tube, which in turn fits into the cell bottom. The steel flange of the cell top is bolted to the

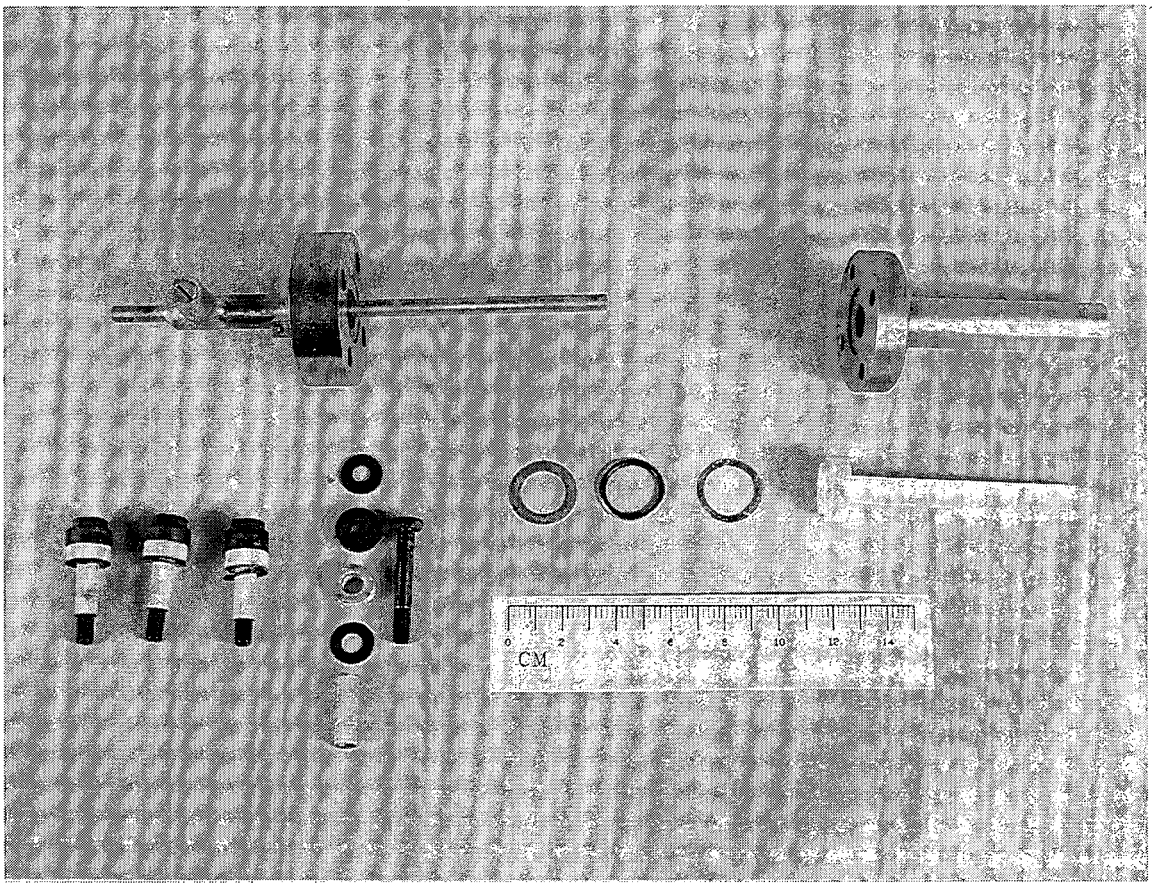

CBB 927-5408

Figure 5. EMF Cell, disassembled.

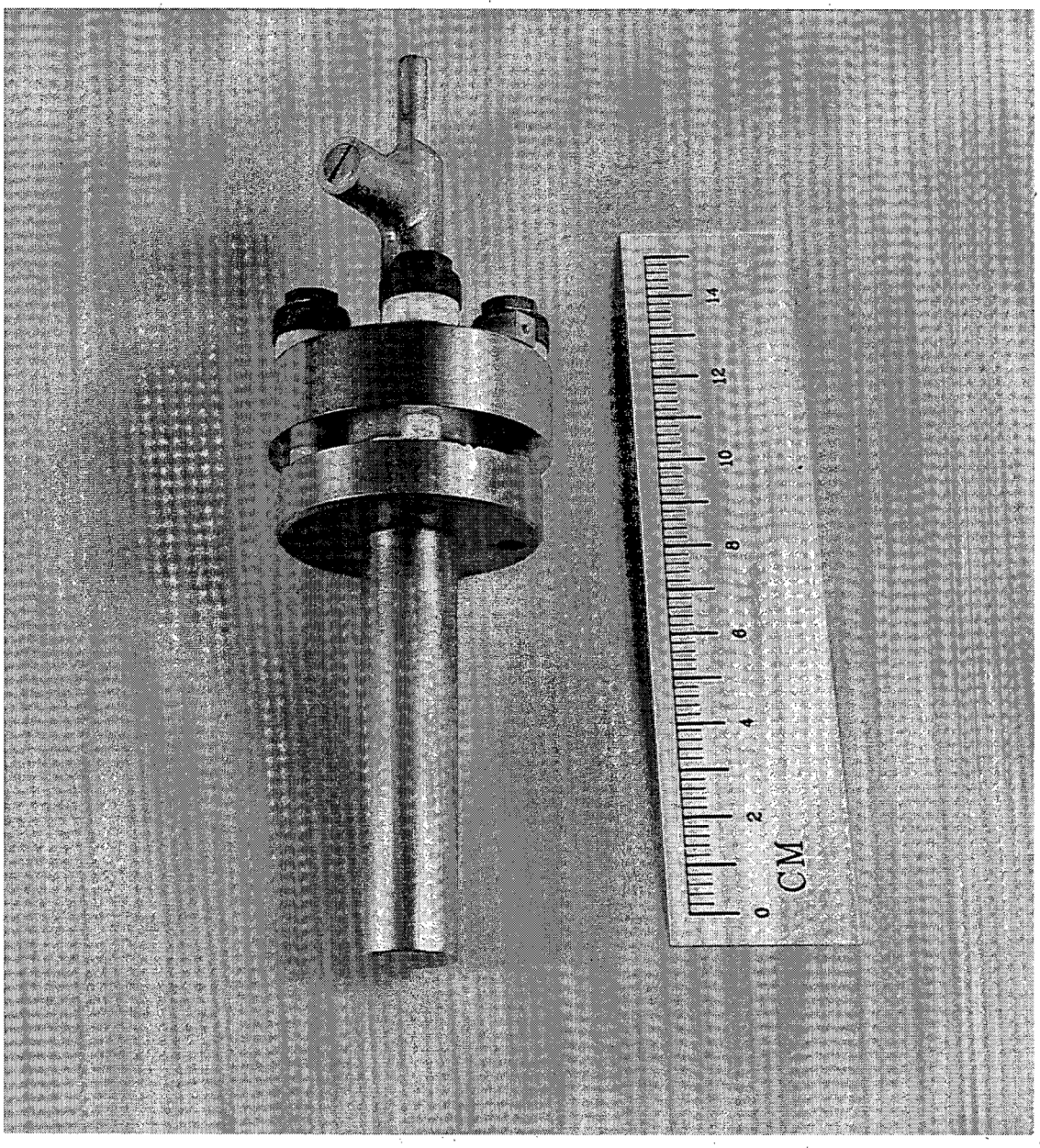

CBB-927-5416

Figure 6. EMF Cell, assembled.

flange of the cell bottom with Type A286 steel bolts, clamping the electrolyte assembly's ceramic collar between the flanges of the cell top and cell bottom. The annular space between the cell bottom and the electrolyte tube is the sodium electrode compartment. The annular space between the electrolyte tube and the current collector tube is the phosphorus-sulfur electrode compartment.

The sodium electrode current collector was the entire cell bottom. The current from this side of the cell was drawn from one of the flange bolts, which were insulated from the cell top by alumina sleeves and spacers. The phosphorus-sulfur electrode current was drawn from a screw set into the cell top flange.

All arc-welded joints (molybdenum-to-molybdenum and steel-to-steel) in the cell were made in an inert atmosphere glove box. The molybdenum weld in the tip of the current collector was stress relieved by heating in a hydrogen furnace to 1800°C for 1 hour to prevent stress corrosion cracking, which had apparently occurred in an earlier prototype after one exposure to sulfur at 350°C. This problem did not recur. However, it was also found that stress relief of molybdenum welds further embrittles these already fragile joints, so no other welds were treated this way.

As an added precaution to minimize the rate of any leak to the outside of the cell[31], the entire furnace-well was pressurized to 100-170 kPa (gauge) to roughly equal the vapor pressure at 500°C of sulfur in the cell. Thus any leakage would be due to diffusion rather than a pressure-driven flow. The efficacy of the C ring, disk springs, and the pressurized furnace-well were not tested separately, so we do not know whether all three are needed together. They are, however, the result of nearly two years of trial-and-error machine-work and learn-by-doing mechanical engineering and metallurgy!

Ancillary Apparatus

During experiments the cell was placed in an ancillary apparatus, shown in Figure 7 with the cell in place, and ready for insertion into the furnace well. The cell fitted into a solid aluminum constant-temperature block. A series of radiation shields were affixed above the block to thermally insulate it in the furnace-well from the glove box floor into which the furnace-well was built. One of the radiation shield support rods guided a thermocouple into the block. This thermocouple was connected to an over-temperature limit switch set to trip at 550°C, safely below the melting point of the aluminum constant-temperature block.

The current from the cell was carried by two Type 304 stainless steel wires encased in quartz tubes which were passed through close-fitting holes in the radiation shields. For the last two experiments[32], 4-wire connections were made to the cell so that polarization data could be obtained without IR drop in the voltage measurement leads. The cell was electrically isolated from the block and heat shield assembly by an assortment of alumina spacers. A photographic detail of the cell installed into the ancillary apparatus is shown in Figure 8. In Figure 9 the ancillary apparatus is being inserted into furnace well in floor of glove box. The furnace insulation is parted and the furnace is opened to show the furnace well.

The furnace-well was sealed off from the glove box with an aluminum lid which allowed the furnace-well to be pressurized to about 15 psig, for reasons described above. The lid was equipped with feed-throughs for the cell terminal leads, and tube connections for a pressure gauge, pressure release valve, and helium gas inlet for pressurization. Figure 10 is a photograph of the ancillary apparatus in place in the glove box, the aluminum lid sealed to the top of the furnace well, all connections made, and ready to run an experiment.

Temperature Control

The cylindrical furnace used to heat the furnace-well employed three independently wired heating elements in a vertical arrangement which surrounded the furnace-well[33]. Though they were controlled by a single temperature controller[34], the total power delivered was divided between them in a constant ratio which had been adjusted to give a uniform temperature (within 1°C at 500°C) along the 8 cm active length of the cell, and a slightly increasing temperature above this region to prevent condensation of sulfur-phosphorus melt in the small spaces above the electrolyte tube.

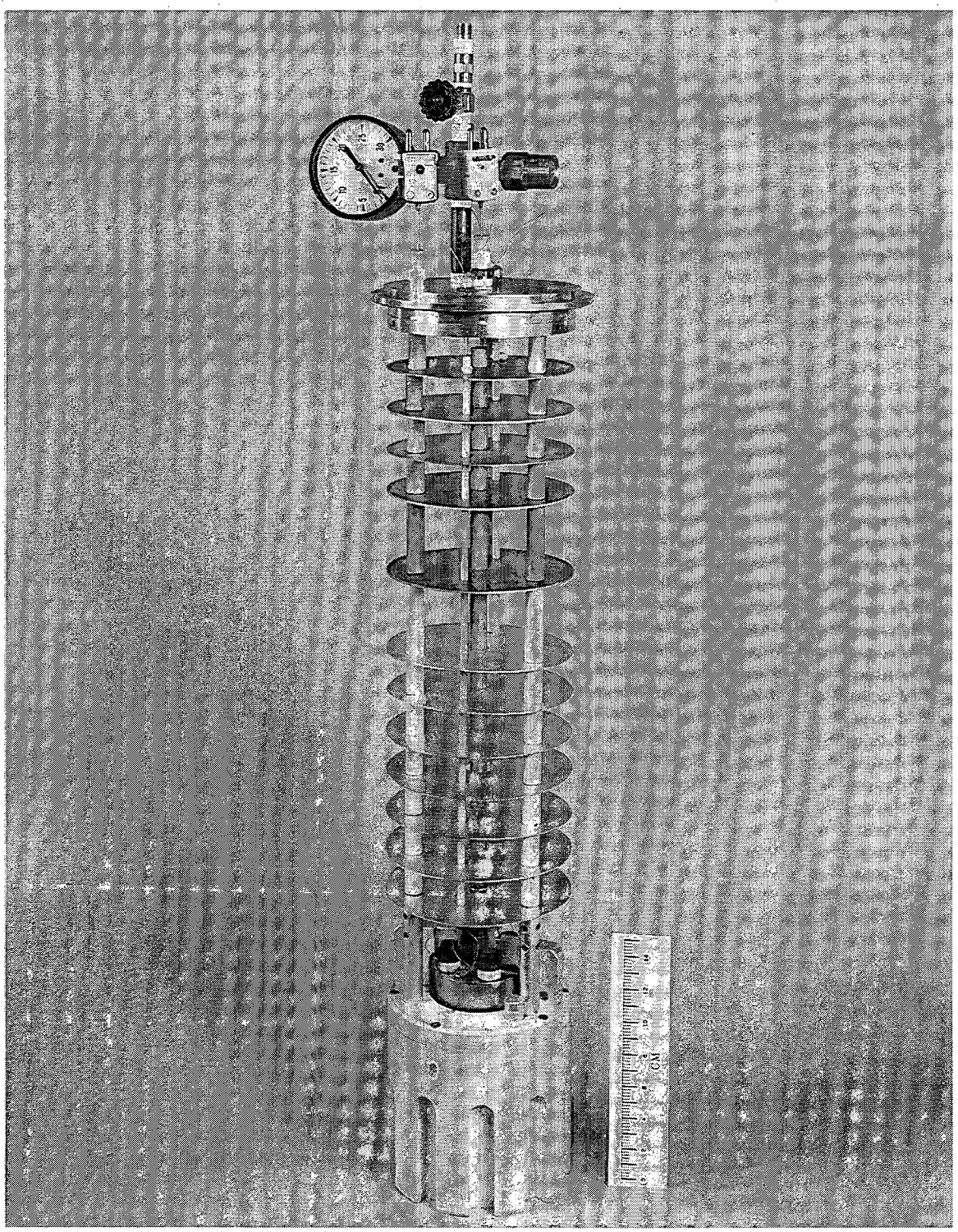

CBB 927-5412

Figure 7. Ancillary apparatus.

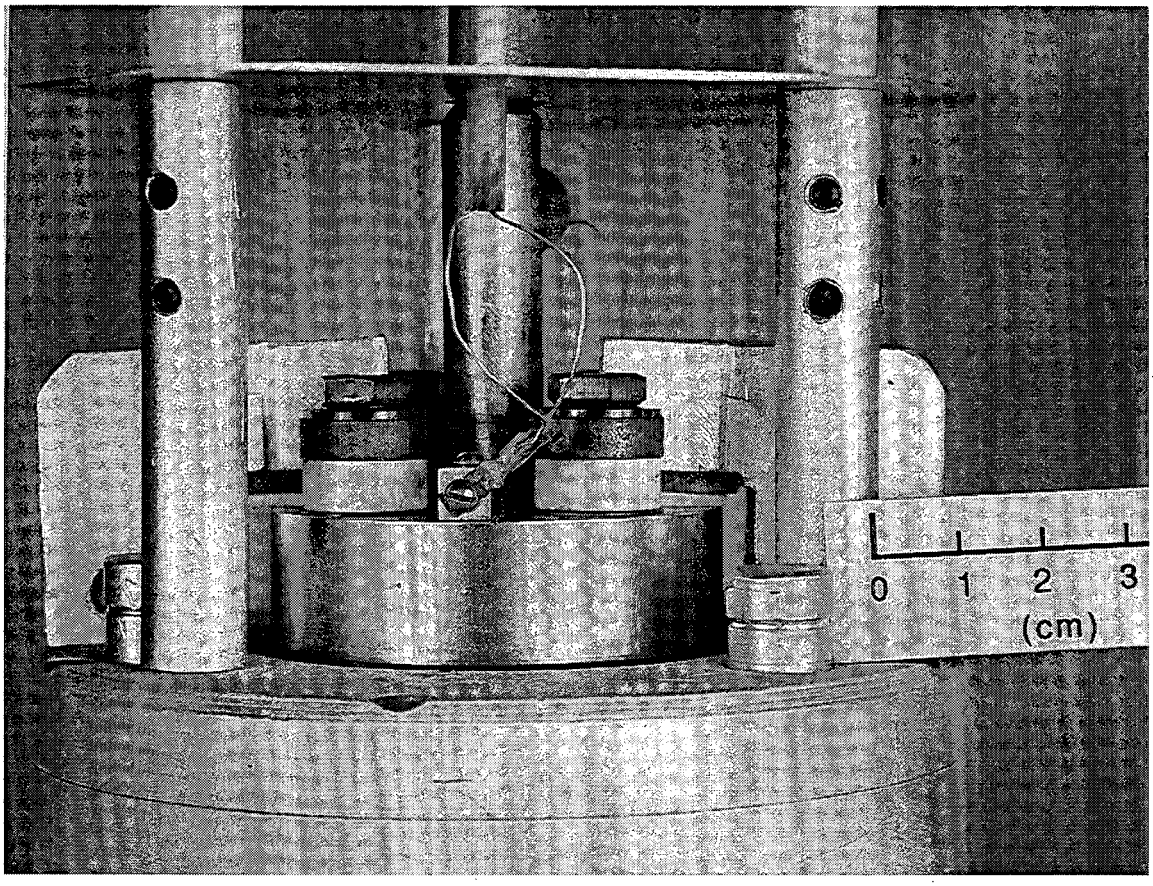

CBB 927-5410

Figure 8. Detail of cell in ancillary apparatus.

CBB 927-5418

Figure 9. Ancillary apparatus being inserted into furnace well in floor of glove box. The furnace insulation is parted and the furnace is opened to show the furnace well.

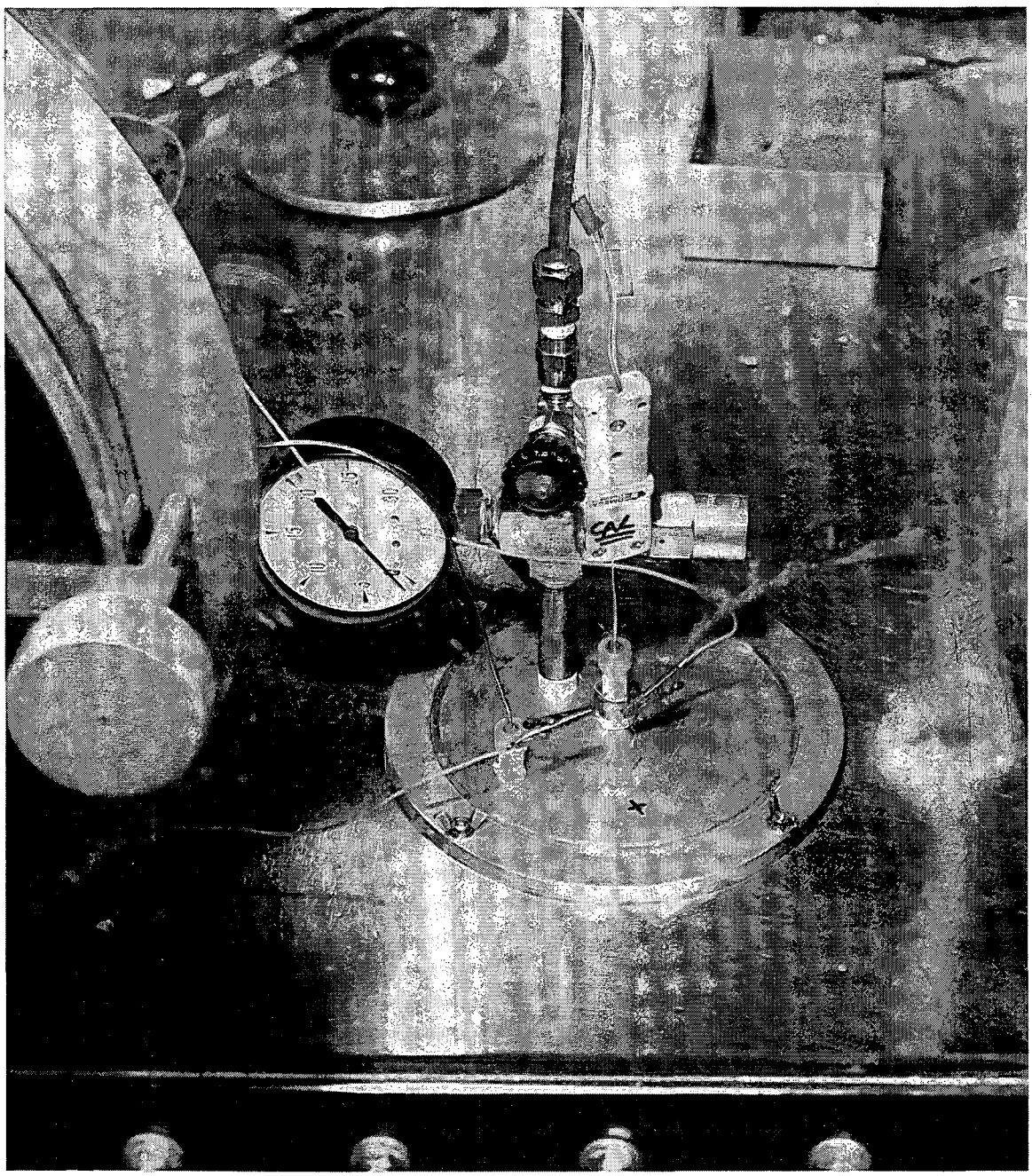

CBB-5414

Figure 10. Ancillary apparatus in place, all connections made, and ready to run.

Electronic Control and Data Acquisition

The current was controlled and the cell potential was measured by a galvanostat equipped with an IEEE digital interface bus[35]. Analog outputs of the cell current and potential from the galvanostat, as well as the cell thermocouple output were monitored by a multi-channel analog-to-digital (A/D) converter[36] which converted the thermocouple voltage to the digitized temperature value, and sent time-stamped voltage, current and temperature data via the IEEE bus to an IBM AT computer[37]. The computer was programmed to operate the galvanostat via the IEEE bus as well as record and display the incoming data. Figure 11 is a schematic diagram of the main components of the experimental system.

The instruments and the computer were mounted into an instrument rack and were electrically isolated from ground and from line power via an isolation transformer. This prevented a ground loop which had allowed a continuous cell discharge of several microamps. The rack was connected to ground through an 80 microfarad electrolytic capacitor to reduce signal noise.

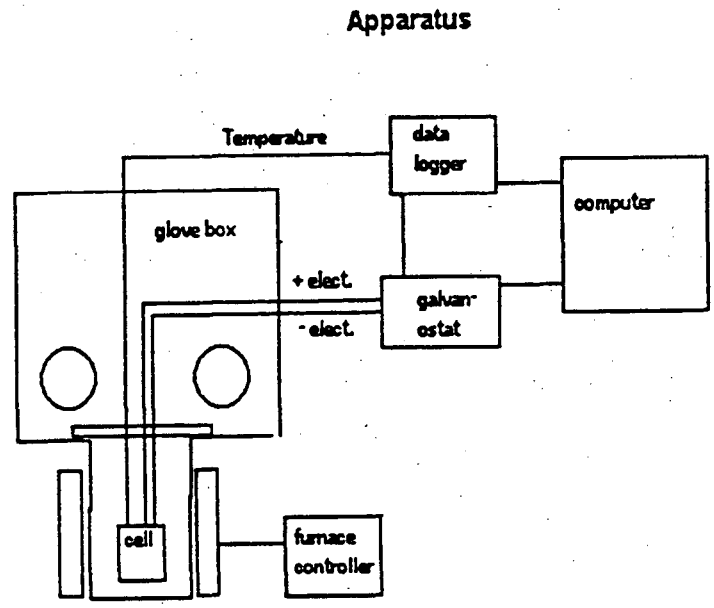

Figure 11. Schematic diagram of the experimental system.

Experimental Procedures

Melting Point Studies

The melting points of various mixtures of sodium, phosphorus and sulfur were determined In a series of glove-box experiments to assess whether and for which S/P ratios the gradual addition of Na would result in mixtures with a low enough melting temperature to allow a cell to operate to a significant depth of discharge at an experimentally accessible temperature. Fourteen mixtures with phosphorus/sulfur ratios

ranging from 0.24 to 1.3 with sodium mole fraction ranging from 0 to 0.6 were prepared from various combinations of P_2S_5, P_4S_3, S, Na_2S, and Na_3P by grinding them together with a mortar and pestle. These powdered samples (@1.25 grams) were then sealed in evacuated pyrex ampoules, and heated in the glove box furnace-well to 400, then 440, then 500°C. The ampoules were removed from the furnace between temperature increments and inspected visually to determine if they had melted.

Though usually it was clear if the sample had melted, occasionally sublimate covered the walls of the ampoule making this determination difficult or impossible. Other samples appeared to separate into discrete components such as a solid and a liquid condensate.

Samples were allowed to equilibrate at a given temperature for at least five hours before inspection. Samples which did not clearly melt by 500°C were then reground in the mortar and pestle, sealed in an ampoule and treated again as above. One sample did melt only after being reground. The results of this study are discussed in the results chapter of this thesis.

The emf cell operates effectively only while the positive electrode is completely molten. Thus these semi-quantitative results were useful in targeting P/S ratios which would allow mapping of liquid phase equilibria deeper into the sodium-rich region of the Na-P-S phase diagram. These same P/S ratios are

also of interest as cathode materials since their tendency to stay liquid in combination with larger quantities of sodium would allow deeper discharges in cells for energy storage.

EMF Measurements

All work described below was carried out in the glove box.

Preparation of the Negative Electrode

Immediately before assembling the EMF cell for an experiment the sodium was put through a final purification step. It was heated to approximately 350°C in a nickel crucible and poured through a plug of stainless steel mesh in a pyrex funnel into another nickel crucible. This removed a surface scum of sodium oxide. Next the sodium was heated with titanium sponge at 350 - 400°C to remove dissolved oxide. Then hot sodium aliquots were transferred into the tared cell bottom via pasteur pipette until it contained the desired weight of sodium, 1.6 - 2 grams.

Preparation of the Positive Electrode

Portions of P_4S_3 (purified as described above), sulfur and carbon black (10 wt-%, to promote conductivity) were weighed

into an agate mortar, ground together thoroughly, and the mixture transferred to the tared electrolyte tube.

Cell Assembly

The cell bottom containing sodium was clamped into an assembly jig. The electrolyte tube was inserted and the cell bottom slowly heated in a crucible furnace until the sodium melted, allowing the electrolyte tube to slide down into place. With the electrolyte tube fully seated into the cell bottom, the cell top was inserted and carefully lowered until the current collector rod touched the still-solid phosphorus-sulfur mixture inside the electrolyte tube. The crucible furnace temperature was then increased until the phosphorus-sulfur mixture melted and the current collector sank into the melt, following which the cell top was seated onto the C-ring seal. The cell top bolts were then inserted and tightened down in a careful sequence so as not to press the tip of the current collector against the electrolyte tube wall. The bolts were finally torqued to 4.5 N-m (40 in-lbs.), securely seating the cell top to the electrolyte assembly header. Then the sulfur electrode compartment was then evacuated and sealed by way of the valve in the cell top.

The cell was then inserted along with alumina insulators into the constant-temperature block. The radiation shield assembly

was affixed to the block, leads connected to the cell terminals, and the entire assembly lowered into the furnace-well. The lid was affixed to the furnace-well which was then pressurized with helium to 100-170 kPa (gauge). Control equipment was connected and heating was begun.

Charge/Discharge Procedure and Data Collection

A computer program for data acquisition and apparatus control was developed to allow the computer to receive time-stamped current, potential, and temperature data from the datalogger while controlling the cell charge/discharge process. It includes a menu-format interface which allows the operator to change system parameters while the program is running. A listing of the source files is included in the appendix. Before the program begins a cell discharge, it records an "equilibrium" cell potential as defined by two parameters: "Dlim" is the maximum value of a function which roughly approximates the magnitude of the time derivative of the cell potential. When a rising or falling cell potential reaches a constant value within the limits defined Dlim, the "equilibrium" data point is recorded. Only then can the program instruct the galvanostat to supply a current to the cell.

For a newly assembled cell initial discharging was done manually. The discharge current was gradually increased from

0.1 mA until at least 1 mA could be sustained with an acceptably low polarization (below 300 mV), at which point the experiment was continued in the automatic discharge mode.

In this mode, the computer is instructed to discharge the cell for a given number of coulombs (counted by monitoring current and time) or optionally, to achieve a given change in sodium mole fraction, before turning off the current and waiting for an equilibrium data point. When the point is taken, the next cell discharge is automatically begun, and the cycle repeated.

To ensure that the data points taken are truly equilibrium values, occasionally the automatic discharge/charge was interrupted, the current direction reversed, and current passed, until the previous value of sodium mole fraction was reached, and an equilibrium data point collected. These checks of equilibrium were performed manually.

Unacceptably large hysteresis observed between data points collected after the passage of current in opposite directions was taken as evidence that equilibrium had not been approached closely enough, and the relevant region of the discharge curve was reinvestigated with tighter equilibration requirements. The amount of hysteresis deemed acceptable depended greatly on equilibration time, which varied from a few minutes to several days.

In the automatic mode, if the cell voltage changes by more than 300 mV during current flow, discharge is stopped, the current setting is decreased, and discharge resumed. Conversely, if after 20 minutes the cell voltage changed by less than 50 mV from the last open circuit voltage the current is increased to save time. As a backup safeguard, a zener diode was connected between the cell electrodes so that the cell voltage could never be forced beyond the range of 0 to approximately 4 volts.

Two data files are created by the program. One, a 'data summary' file contains only equilibrium data. It includes sodium mole fraction, equilibrium cell voltage, total coulombs passed, temperature, etc. This file was used to make plots of equilibrium cell potential versus mole fraction sodium in the phosphorus-sulfur electrode.

The other data file, the 'cell history' file, is a more complete record of data taken once each minute. This file allows diagnosis of system failures and provides a second copy of the information included in the summary file.

Cell Polarization Experiments

Steady-state cell voltage during current flow was measured at states of charge where the equilibrium emf profiles are flat,

in an attempt to get a sense of the current densities obtainable with this system. The polarization experiments were done at sodium compositions near the midpoint of these emf plateau regions, at χ_{Na} = 0.27 and 0.20. Since the passage of current in these experiments did not alter the bulk sodium content by more than 0.02 mole-fraction, the equilibrium emf did not change. Thus the polarization data reflect only the cell internal resistance, uncomplicated by changes in equilibrium emf.

In the experimental procedure, the current was stepped from zero to the desired value and held constant until the emf stabilized, as determined visually with a stripchart recorder. The emf value was recorded, and the current switched off again. The coulombs passed were determined by stopwatch timing of the current steps in early experiments. In later experiments (the Na/S controls) the computer was used to count coulombs.

Cell voltage measurement during current flow is preferably done at points as close to the cell electrodes as possible to avoid inclusion of IR drop in the current-carrying cell-leads in the measurement. As our apparatus was initially designed only to measure voltage in the absence of current, our mid-experiment decision to collect polarization data during emf measurement at P/S = 0.143 resulted in the inclusion of the

effect of the relatively high resistance of the two stainless steel cell leads which were used both to carry current and measure voltage. After the experiment was terminated, the resistance in the cell leads was independently measured by connecting the ends which were attached to the cell to each other, heating them in the furnace well and measuring the resistance with an ohmmeter at 350 and 400°C.

For each polarization data point, an IR drop due to this resistance and the current at that data point was calculated and subtracted from the cell voltage giving an IR-corrected polarization curve. These corrected data are appropriate for comparison with the sodium/sulfur polarization data which were collected later in an apparatus modified by the addition of two more cell leads to allow voltage measurement without the IR drop present in the current-carrying leads.

Cell Disassembly

Following an experiment, after the ancillary apparatus cooled to below 200°C, it was removed from the furnace well, disassembled, and the cell was removed from the constant temperature block. Usually the electrolyte tube had broken and the electrode materials had fused together. Separation of the cell top from the cell bottom usually required heating the cell bottom in a crucible furnace to 300-400°C while trying to

pull the two halves of the cell apart. The cell parts were then cleaned with water, methanol, and acetone, and dried with compressed air and vacuum before reassembly. Several times the surface of the molybdenum sealing disk appeared warped after an experiment, and was re-machined to flatness. The C-rings, which were supposed to be re-usable, tended to remain partially compressed after one use. Several were used a second time without apparent leakage.

One of the purposes of the cell design was to re-use electrolyte tubes for more than one experiment. In retrospect, it would be difficult to get repeatable performance from one experiment to the next because of the difficulty of adequately cleaning the tubes. No solvent was found which could remove the sodium stain from the tube or dissolve the positive electrode material from a partially discharged phosphorus/sulfur electrode.

Results

The results of the experimental work and analyses of the data are presented in this chapter.

Melting Point Studies

As cell discharge experiments are possible only when the electrodes are liquid, we attempted visual determination of the melting point of several sodium-sulfur-phosphorus mixtures, via the method described in the experimental section of this thesis. This was intended as a relatively quick, qualitative study to identify compsition ranges which are liquid below 500°C.

The results, shown graphically in Figure 12, indicate that mixtures with P/S ratios greater than 0.5 and sodium atom fraction (χ_{Na}) greater than 0.2 are solid below 500°C. The sulfur electrode in a standard Na/S cell is routinely discharged to χ_{Na} = 0.4 at 350°C because such Na-S mixtures are liquid up to this sodium composition at this temperature; a competitive P/S electrode will have to be similar or better in this characteristic. Thus phosphorus will probably be the minor constituent in an optimized P-S electrode.

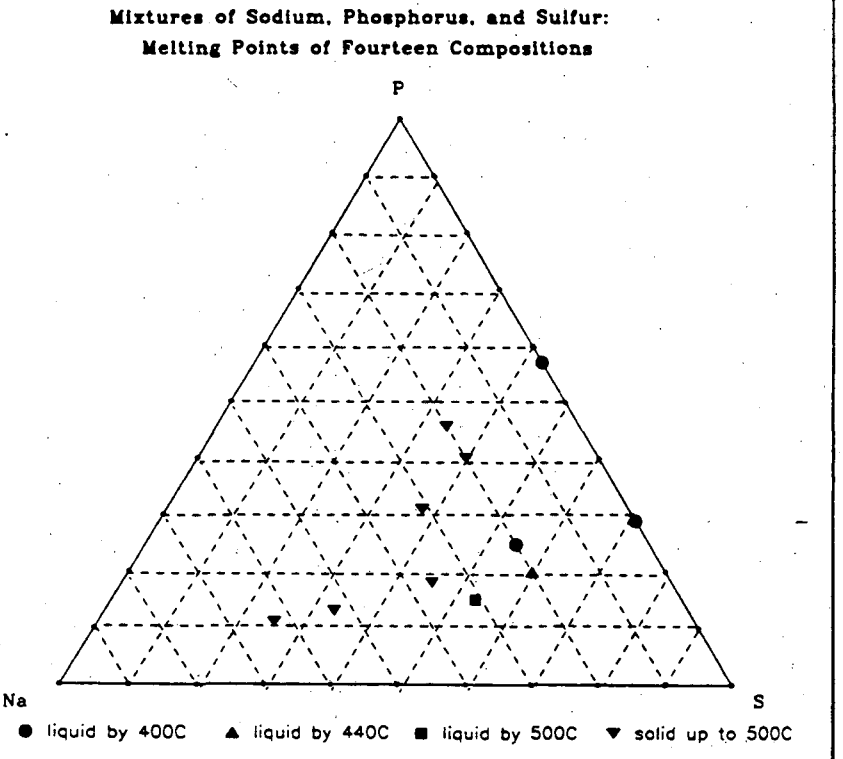

Figure 12. Results of melting point study.

The published Na_2S - P_2S_5 phase diagram[9] shown in Figure 3 agrees well with our melting point results for the two compositions which were made from mixtures of Na_2S and P_2S_5, as shown in Table I. This supports our results, which roughly indicate that cell emf measurements are possible below our temperature limit of 500 °C up to nearly χ_{Na} = 0.4 with P/S ratios below 0.4.

Table I: Comparison of melting point data with reference (9).

composition ($\chi_{Na}, \chi_P, \chi_S$)	lit. m.p. (°C)	our m.p. (°C)
0.2, 0.2, 0.6	@ 430	400 < m.p. < 440
0.31, 0.15, 0.54	@ 450	440 < m.p. < 500

EMF Studies

Equilibrium cell emf measurements were performed using four different positive electrode compositions, three of which were phosphorus-sulfur mixtures. A control experiment using only sulfur as the positive electrode was carried out at 350 and 400°C. Figure 13 shows that the data at 350°C agree closely with data from the literature[38]. Figure 14 shows the 400°C Na/S cell data along with the few published data for this cell at this temperature[38].

Three phosphorus:sulfur ratios were investigated at temperatures ranging from 350 to 500°C. Due to the long equilibration times and the short life of the electrolyte assembly at the higher temperatures (400+ °C), the full temperature range accessible to the apparatus could not be investigated before the cells failed. The results are displayed along with the emf curve for the Na/S cell to show the range over which the phosphorus-sulfur electrode gives a higher equilibrium emf.

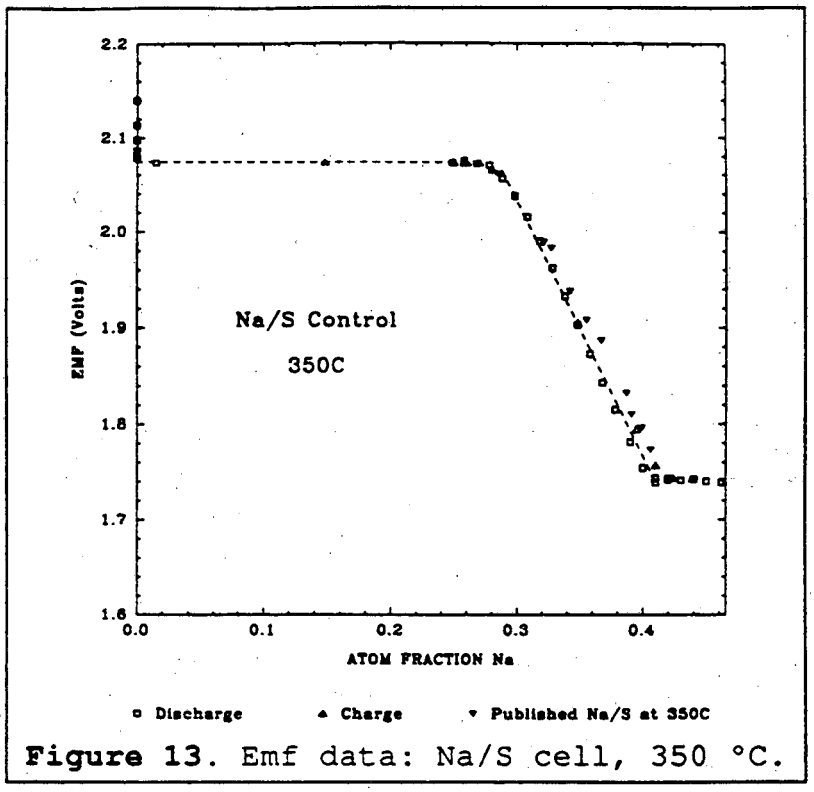

Figure 13. Emf data: Na/S cell, 350 °C.

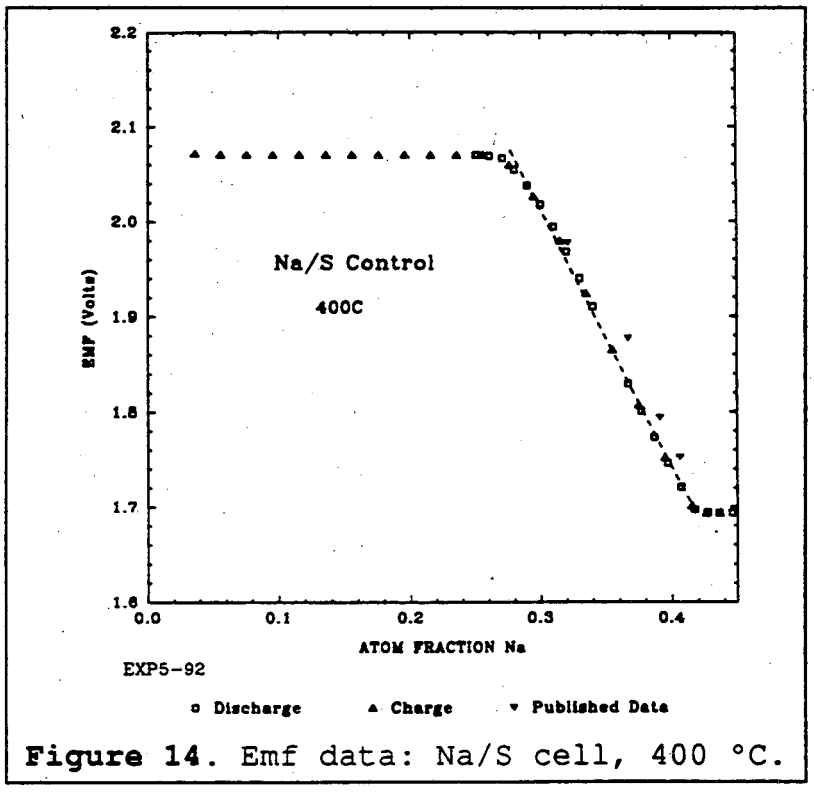

Figure 14. Emf data: Na/S cell, 400 °C.

Na-P/S Cell, With P/S = 0.143

This was the longest-lived experiment at 50 days, terminated by electrolyte failure (cracking). In that time data were collected at 350 and 400°C. Plots of EMF versus sodium atom-fraction (χ_{Na}) are shown in Figure 15 and Figure 16. At both temperatures, these cells were discharged successfully until χ_{Na} in the positive electrode reached more than 0.4, which for sodium/sulfur cells is the usual discharge limit. At this point, equilibration times grew to several days, so that gathering data at higher χ_{Na} values became impractical. Note that the data gathered on charge gives higher emf values. This is an expected hysteresis due to the long equilibration times (up to about two days per point) required in a practical experiment. The true equilibrium emf should be within the range shown by the hysteresis between the discharge and charge data. An exception is the disparity between the charge and discharge data in the plateau region at about χ_{Na} = 0.2 at 350°C (Figure 15). The higher plateau may be due to the development of a meta-stable phase upon charge. Note that at 400°C (Figure 16) the higher plateau disappears.

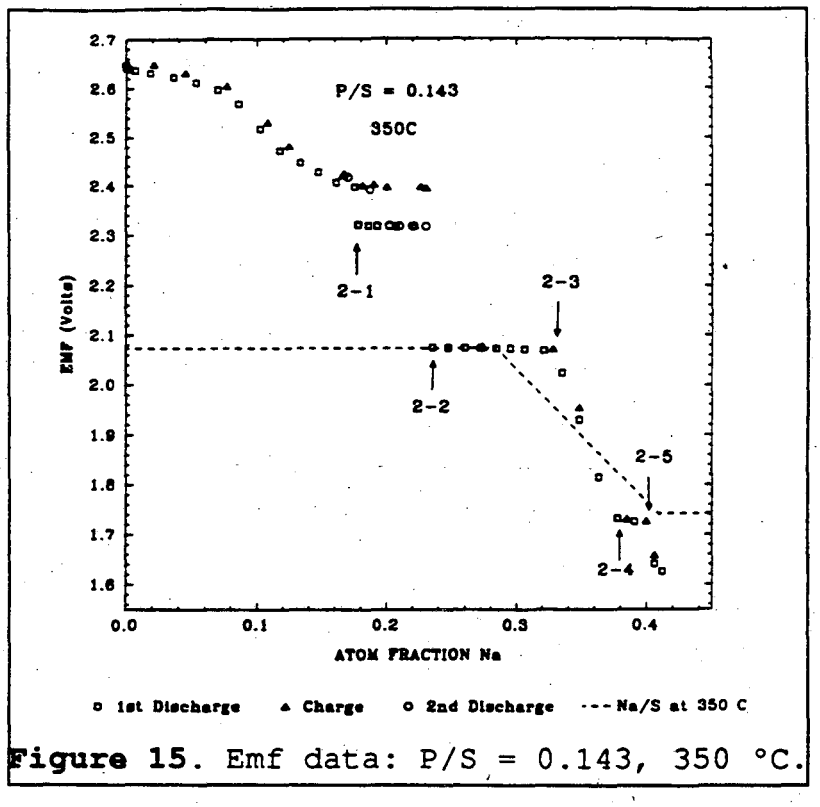

Figure 15. Emf data: P/S = 0.143, 350 °C.

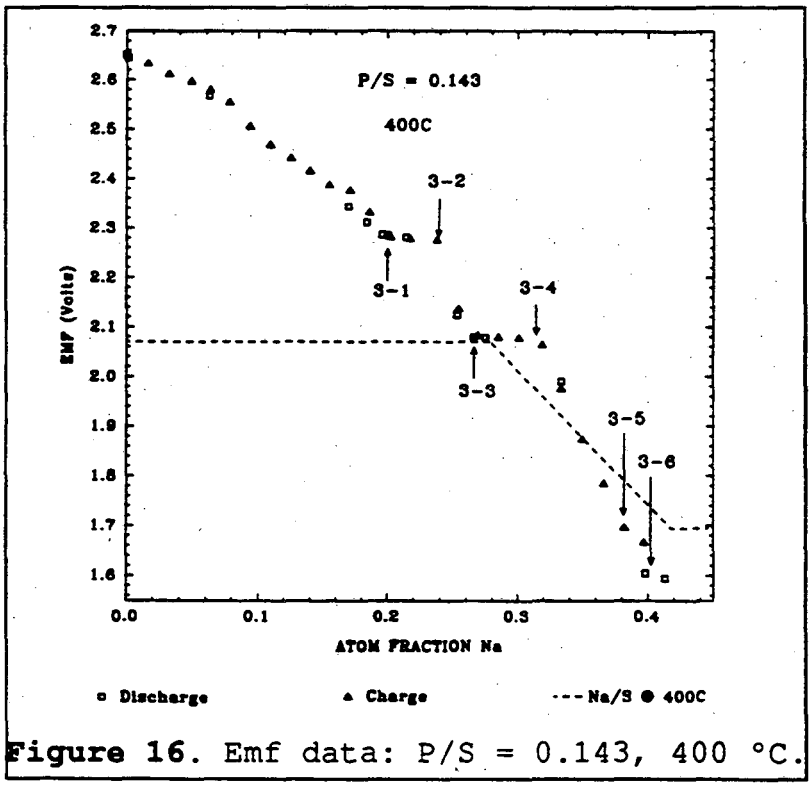

Figure 16. Emf data: P/S = 0.143, 400 °C.

Na-P/S Cell, With P/S = 0.332

This experiment was attempted at 350°C, but discharge rates were so low and equilibration times were so long (probably due to formation of solids or very viscous material) that only a few irreproducible data points were collected and are not shown here.

At 400°C the cell discharged more readily up to χ_{Na} = 0.264, after which an abrupt plunge in potential coincided with a large increase in equilibration time making further discharge impractical. These data are shown in Figure 17. The electrolyte tube failed before higher-temperature data could be collected.

Na-P/S Cell, With P/S = 1.17

This atom ratio was chosen in spite of the melting point data because it is very close to a 115 °C P-S eutectic (in the absence of sodium). In agreement with our melting point data, however, low allowable discharge rates and long discharge times at temperatures up to 500°C suggest that highly viscous materials (if not solids) were being formed in the cell as the χ_{Na} reached 0.14. The data are shown in Figure 18.

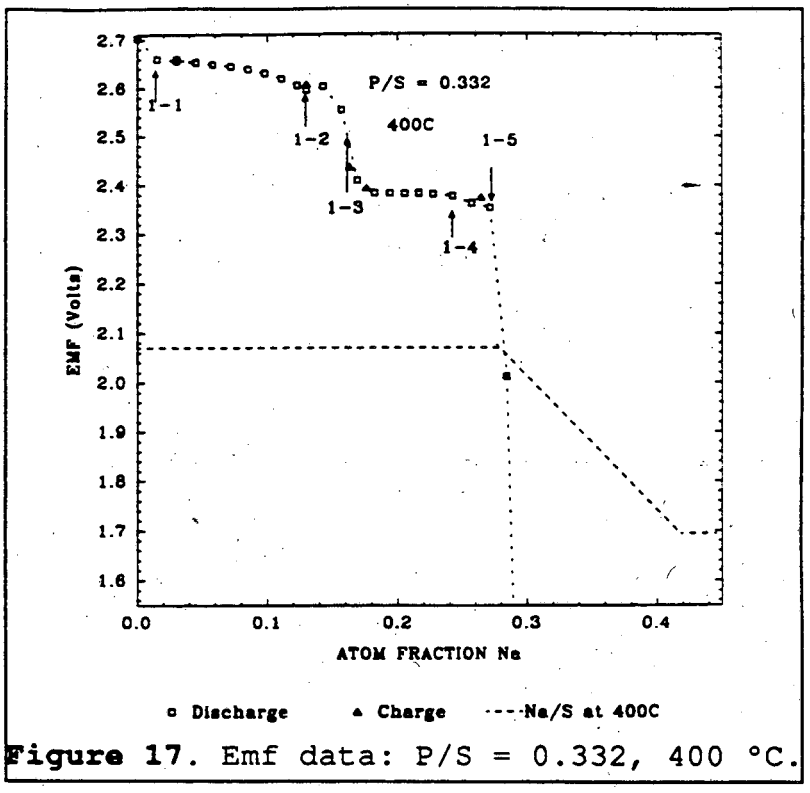

Figure 17. Emf data: P/S = 0.332, 400 °C.

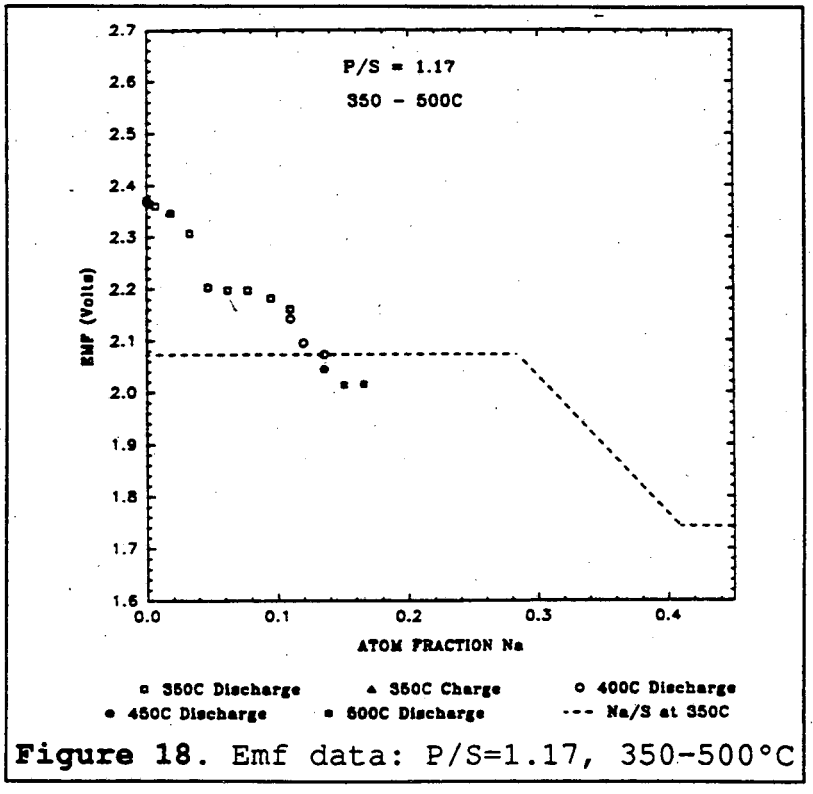

Figure 18. Emf data: P/S=1.17, 350-500°C

Reproducibility of Emf Data

The limits of reproducibility of equilibrium emf versus χ_{Na} measurements are shown by the hysteresis between the charge and discharge data. This hysteresis may be solely due to a "maximum" error in equilibrium emf measurement, a maximum error in χ_{Na} calculation, or a combination of smaller errors in both. The emf uncertainty limits the precision of the estimate of the specific energy of the cell. The uncertainty in χ_{Na} affects our ability to precisely locate phase-field boundaries.

An example of the error estimation method using data from Figure 15 is represented in Figure 19. The two data points which are nominally at $\chi_{Na} = 0.348$ are in disagreement. If we assume that the χ_{Na} value is correct, the disagreement is wholly due to error in emf measurement, giving a maximum emf error of ± 12 mV.

If the emf measurements are assumed to be correct, the data in Figure 19 can be used to calculate a maximum error in χ_{Na}. This is only possible because there are enough discharge data points in the immediate area to be able to interpolate discharge data reliably[39]. As shown in Figure 19, the magnitude of the χ_{Na} uncertainty is the difference between the χ_{Na}

value of the charge data point and that of the interpolated discharge data point at the same emf value.

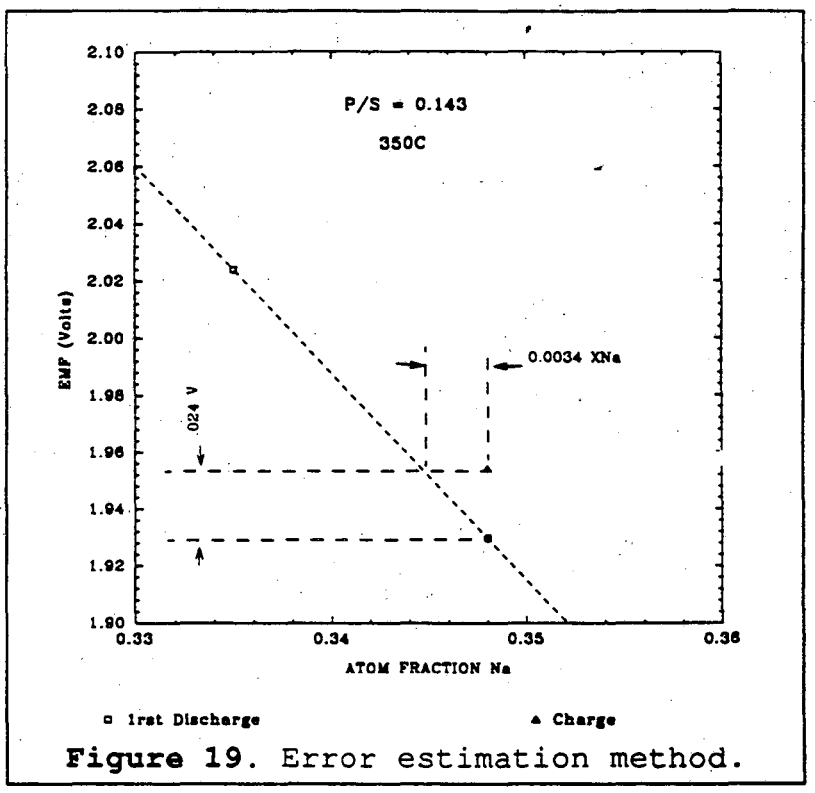

Figure 19. Error estimation method.

In general, data hysteresis could be due to combined error in emf and χ_{Na} where the error in each is less than the values calculated as shown in Figure 19. However, it is prudent to consider these maximum errors as the independent uncertainties in χ_{Na} and in emf. Since the hysteresis is much less in the regions of zero slope in the emf plots, a separate emf uncertainty is calculated for these regions.

The standard deviations of the emf reproducibility (summed with the instrumental uncertainty in emf measurement of ±0.2 mV, std. dev.) and of the uncertainty in χ_{Na} are shown in Table II. Each entry in Table II is the result of the above error analysis on a pair of data points with the same χ_{Na} value, one taken on charge and the other on discharge.

Table II: Error estimates.

Experiment	$\Delta\chi_{Na}$	Δemf sloping region (±,mV)	Δemf plateau region (±,mV)
P/S = 0.143 350°C	±0.0017	12 9	4.5 6.5 2
P/S = 0.143 400°C		7 17 10.5	1.5 0.7 10.8
P/S = 0.332 400°C	±0.00001	0.3	6 6
P/S = 0 350°C	±0.00025		
STD. DEV.	±0.001	10	4

Theoretical Specific Energy

The emf data were used to calculate the theoretical specific energy via the method described in the introduction chapter of this thesis. The results are shown in Table III.

Note that the specific energy of the P/S = 0.143 cell is 11% higher than that of the Na/S control experiment, at both 350 and 400°C. The specific energy of the P/S = 0.332 cell is 25% less than that of the Na/S control cell.

Table III: Specific energy.

Cell Type	P/S (mole ratio)	Temp (°C)	Sp. E. (W-hr/kg)
Na/S[40] (lit)	0	350	767
Na/S	0	350	770
Na/S	0	400	758
Na/P-S	0.143	350	825
Na/P-S	0.143	400	820
Na/P-S	0.332	400	571

Experimental Determination of n

An important aspect of the nature of the cell reaction, the *number of electrons* (n) *transferred per mole of reaction product formed*, can be obtained from equilibrium emf data, as discussed in the introduction chapter of this thesis. EMF data from the sodium/sulfur control experiment at 350°C were collected in the extremely narrow composition range (χ_{Na} = 0 to 0.00013) of the low-sodium single-phase region to test our ability to measure n. The requisite plot of cell emf versus $\log(\chi_{Na})$ is shown in Figure 20. The slope ($dE/d(\ln\chi_{Na})$) obtained was -0.0256 which, via

$$\frac{dE}{d\ln(\chi_{Na})} = -\frac{RT}{nF}$$

(see the introduction chapter) corresponds to an n of 2.09, quite close the expected value of two[41].

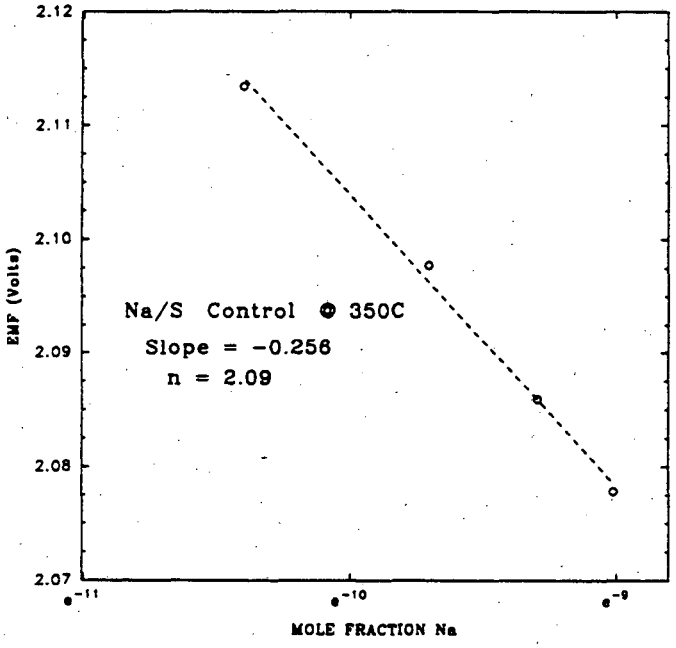

Figure 20. Emf vs. log χ_{Na}, Na/S cell.

If one of the known sodium phosphides (NaP[42], NaP_{15}[43], Na_3P, Na_3P_7[44], Na_3P_{11}[45], Na_3P_{21}[46]) is the single reaction product in the nearly fully charged phosphorus-sulfur electrode, n would be 1 or 3, and the corresponding slope of a plot of EMF versus

$\ln(\chi_{Na})$ should be found. Cell emf data were collected at very low χ_{Na} for P/S = 0.143, 0.332, and 1.17. In each case the log plot was not linear, and attempts to estimate n from these plots resulted in values ranging from 0.1 to 40. This is surprising since the measurement seemed so definitive in the control experiment. Impurities within the cathode melt, perhaps the result of corrosion reactions at the high cell emf (compared to Na/S), may have caused this unexpected behavior.

Emf Studies - Conclusions about Cell Performance

The EMF data indicate that addition of up to 12 mole % phosphorus (i.e. P/S mole ratio 0.143) could improve the sulfur electrode. Thus this phosphorus:sulfur ratio was chosen for further study via cell polarization measurements.

In comparison, addition to the positive electrode of over 25 mole % phosphorus (P/S = 0.332 and 1.17) gives both lower open circuit voltages and a large increase in cell resistance, as manifested by the high overpotentials observed when passing current through the cell. The high cell resistance at P/S = 0.332 is not surprising as mixtures of P_2S_5 (P/S = 0.285) and Na_2S are known to form glass-like (i.e. highly viscous) systems[11].

Cell Polarization Data

The promising results obtained during the emf study at P/S = 0.143 motivated the collection cell voltage versus current (polarization) data during that experiment. This necessitated the collection of polarization data during the sodium/sulfur control experiment for comparison.

Figure 21 and Figure 22 show plots of current density versus cell voltage (polarization data) for the P/S = 0.143 experiment at 350 and 400°C, along with the results of the same measurements on the sodium/sulfur control cell. The sulfur-phosphorus electrode gave lower voltages on discharge and higher voltages on charge than the pure sulfur electrode over the entire current range tested, indicating that under these conditions, phosphorus appears to degrade cell performance.

Closer examination of the polarization data reveals two characteristics of the phosphorus-containing electrode, neither of which occur in the pure sulfur electrode, and both of which produce the poor cell performance. One is a charge - discharge hysteresis in the data collected at χ_{Na} = 0.20, and the other is a higher resistance in the cell with the P-S electrode, at both χ_{Na} 0.2 and 0.27.

Charge-Discharge Hysteresis

The equilibrium emf studies at P/S = 0.143 (Figure 15 and Figure 16) show an upper emf plateau at about 2.3 volts and a lower one at 2.1 volts. In Figure 21 (350°C) the discharge and charge curves recorded at χ_{Na} = 0.27 extrapolate to 2.07 volts (the equilibrium open-circuit emf) at zero current, as expected. At χ_{Na} = 0.20 the equilibrium EMF is about 2.32 volts, so one might expect the polarization curve to pass through zero current at 2.32 volts. The charging curve does. However, the discharge curve at χ_{Na} = 0.20 appears to extrapolate to 2.07 V at zero current. One explanation is that even very low discharge current densities cause coating of the electrolyte with a sodium-rich film in the composition range defined by the 2.07 volt plateau in Figure 15 and Figure 16.

Figure 22 contains plots of polarization data for the P/S = 0.143 experiment at 400°C. The plot at χ_{Na} = 0.27 behaves in the simple expected fashion as it did at 350°C. In the plot at χ_{Na} = 0.2 hysteresis was observed, as it was at 350°C. Two sets of discharge data were collected with one set of charge data collected between them. In the charging data, the first two data points extrapolate to 2.08 V at zero current instead of the true equilibrium value of 2.3 V at this bulk electrode composition. This is the effect of the discharge which immediately preceded the collection of the charge data - the

coating of the current collector with a material of higher sodium content than exists in the bulk electrode. Note that since the two charging data points at higher current densities extrapolate to about 2.28 V at zero current, apparently the effect of the previous discharge had been eliminated. The discharge was then repeated. The first discharge current data point, taken immediately after the charging data, appears to be associated with a 2.3 V emf at zero current: At this point the non-equilibrium coating had not formed. But the rest of the second discharge data extrapolate to 2.08 V at zero current, indicating that the sodium-rich coating had reformed.

In summary, over the composition range of the upper voltage plateau, this cell behaved, on charge, as if it had a higher open circuit voltage than on discharge. This charge/discharge hysteresis is not advantageous from the standpoint of energy storage, as it corresponds to an inherent energy inefficiency which does not exist in competing systems, such as the Na/S cell.

On the other hand it is important to remember that these polarization measurements have tested cell performance only at two specific electrode compositions, χ_{Na} 0.2 and 0.27. In practical use the positive electrode would be charged and discharged over compositions ranging from $0 < \chi_{Na} < 0.4$ and this hysteresis may occur only over a small portion of the

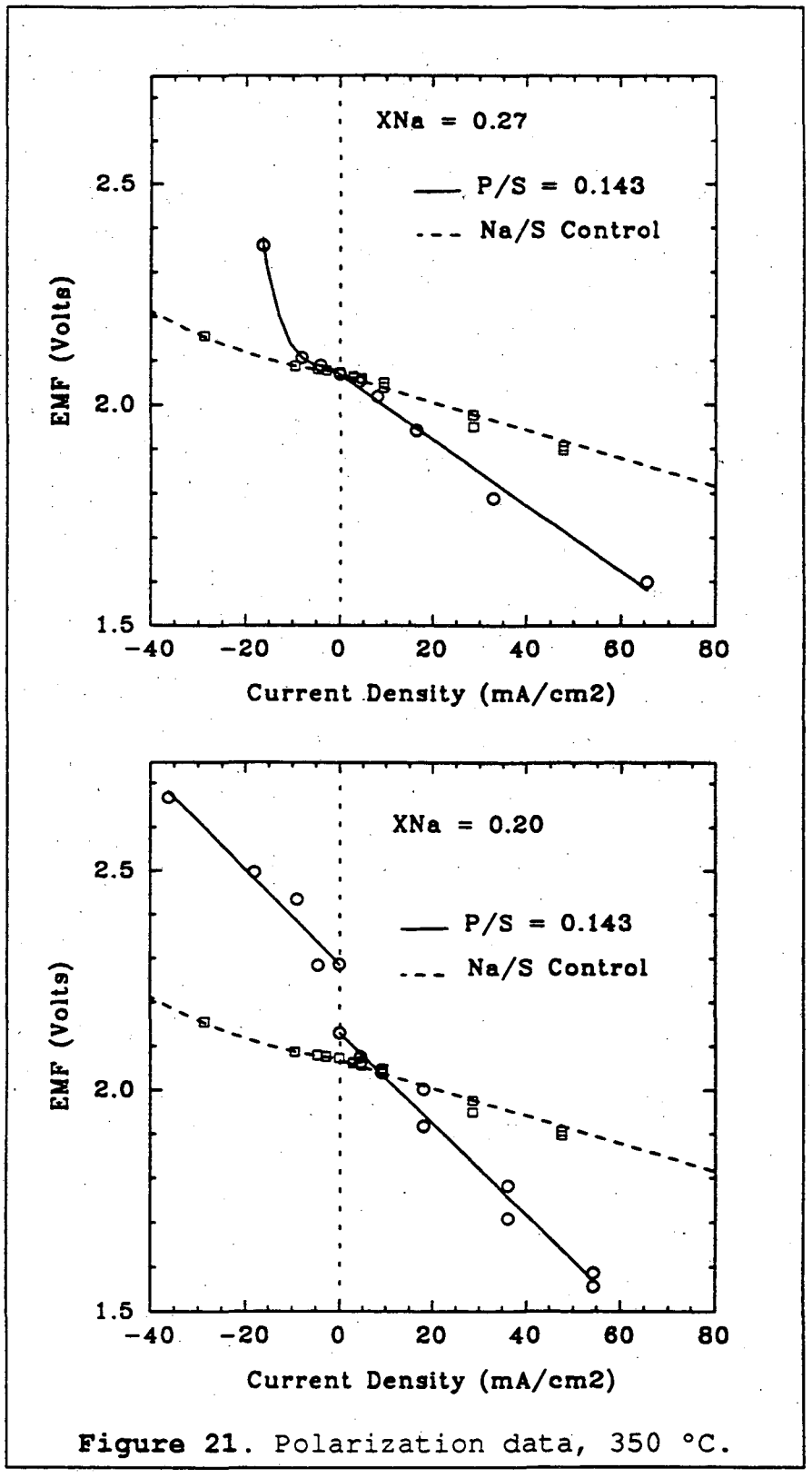

Figure 21. Polarization data, 350 °C.

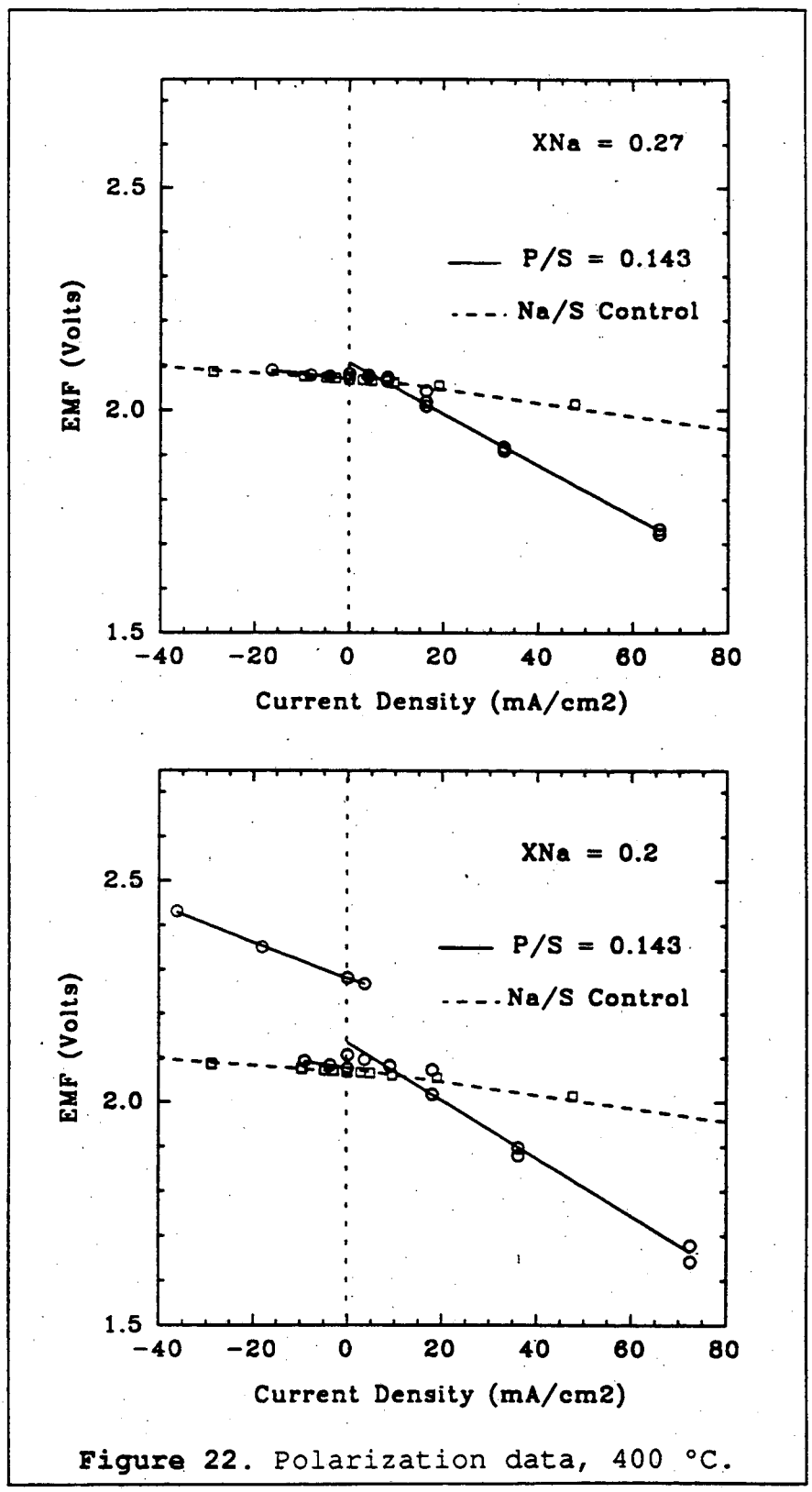

Figure 22. Polarization data, 400 °C.

charging curve. The overall energy efficiency of a complete charge/discharge cycle at substantial current densities would be a more conclusive measure of cell performance for battery purposes.

Cell Resistance

The polarization data for P/S = 0.143 and the sodium/sulfur control experiment include the effect of internal cell resistance, which causes the polarization plots to have a non-zero slope. This includes ionic resistance in the positive electrode melt and in the electrolyte, and also the effect of concentration gradients in the positive electrode.

The lower the internal cell resistance, the better the cell performance. The cell resistance obtained using a phosphorus-sulfur electrode can be compared to the resistance of the same cell using a sulfur electrode as an indicator of the relative performance of these electrode materials. Table IV gives this comparison. The most significant result is that the resistance of the sodium/P-S cell was two to four times larger than that of the sodium/sulfur cell.

Two other trends are that cell resistance decreases with increased temperature (as expected) and that there is less

resistance on discharge from the 2.07-volt plateau (χ_{Na} @ 0.27) than from the 2.32 volt plateau (χ_{Na} @ 0.20).

Table IV: Cell internal resistance.

P/S (mole ratio)	Temp (°C)	χ_{Na}	Current Polarity	Rcell (Ω)
0 (Na/S ctrl)	350	0.15	chg	1.5 - 4.2
0.143	"	0.27	chg	3.1 - 4.3
0.143	"	0.20	chg	11.0
0	"	0.15	dchg	3.0
0.143	"	0.27	dchg	7.4
0.143	"	0.20	dchg	10.3
0	400	0.15	chg	0.73
0.143	"	0.27	chg	1.1
0.143	"	0.20	chg	4.1
0	"	0.15	dchg	1.5
0.143	"	0.27	dchg	5.7
0.143	"	0.20	dchg	6.5

Cell Polarization Studies - Conclusions

Figure 21 and Figure 22 show that the cell containing phosphorus is inferior to the sodium sulfur cell in performance. At any given current value in the range studied, the phosphorus-sulfur electrode delivers less power on discharge, and requires more power on charge. It is important to note that the polarization behavior of a single P/S ratio has been

tested only at two compositions, χ_{Na} = 0.2 and 0.27. It may be that this electrode performs better at other states of charge, and also that another P/S ratio (probably less than 0.143, given the emf data for P/S = 0.332 and 1.17) might give better performance. By similar reasoning, the results of the cell resistance comparison are not conclusive.

As discussed in the introduction, there is reason to expect phosphorus to improve the charging characteristics of the nearly fully charged cell. Also, the higher open-circuit voltages (compared to Na/S) at positive electrode compositions $\chi_{Na} < 0.18$ may give better power output than the Na/S cell. A conclusive cell performance test would be a series of constant-current cell discharges and charges, covering the full capacity of the cell and a range of current densities, compared to the result for the Na/S control.

Unfortunately the lifetime of the cells with P-S electrodes has not been long enough to do this important series of experiments. Also P/S ratios between 0 and 0.143 have not been tested, and may give better results. It is conceivable that a phosphorus content in this range may act as a sodium polysulfide or sulfur chain terminator, thereby reducing viscosity, without forming a highly viscous glass-like system which is reported for higher phosphorus concentrations in mixtures with sulfur and sodium.

Phase Equilibria

The EMF data have also been used to begin to determine the phase diagram of the Na-P-S system at 350 and 400°C. No ternary diagram has been published for this system, and only one of several possible pseudo-binary diagrams, the Na_2S - P_4S_{10} phase diagram reproduced in Figure 3, has rewarded a thorough literature search[9].

The ternary diagrams proposed here are based on a small amount of data, plus phase-rule considerations. An attempt has been made to explain the experimental and published data with as simple a system of equilibria as possible, while obeying the laws of thermodynamics.

As discussed previously, a break in the slope of a plot of cell emf versus χ_{Na}, and/or discontinuities in the plot, indicate the crossing of a boundary between phase fields. It is useful to classify slope breaks as one of four types. They are transitions from:

(Type 1) one non-zero slope to another non-zero slope

(Type 2) a non-zero slope to a zero slope

(Type 3) a zero slope to a non-zero slope

(Type 4) a zero slope to another zero slope at a different cell emf

Table V: Phase boundaries from cell emf data.

I.D. #	P/S ratio	Temp (°C)	χ_{Na}	χ_P	χ_S	Type
1-1	0.332	400	0.015	0.245	0.740	1
1-2	0.332	400	0.130	0.217	0.653	1 or 2
1-3	0.332	400	0.17	0.207	0.623	4
1-4	0.332	400	0.242	0.189	0.569	3
1-5	0.332	400	0.270	0.182	0.548	-
2-1	0.143	350	0.179	0.103	0.718	2
2-2	0.143	350	0.238	0.095	0.667	4
2-3	0.143	350	0.330	0.084	0.586	3
2-4	0.143	350	0.380	0.078	0.542	1
2-5	0.143	350	0.400	0.075	0.525	-
3-1	0.143	400	0.200	0.100	0.700	2
3-2	0.143	400	0.240	0.095	0.665	3
3-3	0.143	400	0.270	0.091	0.639	2
3-4	0.143	400	0.320	0.085	0.595	3
3-5	0.143	400	0.382	0.0773	0.541	1
3-6	0.143	400	0.400	0.075	0.525	1 or 2

The relationship between the slope of the emf vs. χ_{Na} plot and phase behavior discussed in the introduction chapter results in the following interpretation of these types of breaks in slope: A "Type 1" transition is from a single- (or two-) phase region to a two- (or single-) phase region. A "Type 2" transition is probably from a two-phase region to a three-phase region. A "Type 3" transition is from a three-phase

region to a two-phase region. A "Type 4" transition is from one three-phase region to another three-phase region. The breaks in slope in the emf data are marked and labeled for reference in the cell emf vs. χ_{Na} plots (Figure 15 through Figure 18), and listed in Table V.

The entire Na-P-S ternary diagram is triangular in shape. It is shown, along with various known compounds and their melting points, in Figure 23. Because the data to be presented here lie in the sulfur-rich corner of the diagram, the indicated region is expanded in subsequent figures.

The 350°C Ternary Phase Diagram

A partial isothermal section of the Na-P-S ternary phase diagram is proposed in Figure 24 for 350°C and in Figure 25 for 400°C. Plotted in these diagrams are compositions of known compounds which are solid, and compositions where phase transitions are known to occur along the Na-S binary axis. The phase transitions from the Na_2S - P_4S_{10} pseudo-binary diagram, labelled a through e in Figure 3, are also shown in Figure 24 and Figure 25. Phase transitions inferred from the cell emf data, labelled in Figure 15 through Figure 17, and listed in Table V, are also plotted in Figure 24 and Figure 25. The data from the experiment with P/S = 1.17 was not considered as the composition of this electrode places the

resulting data in a part of the diagram distant from the rest of the available information.

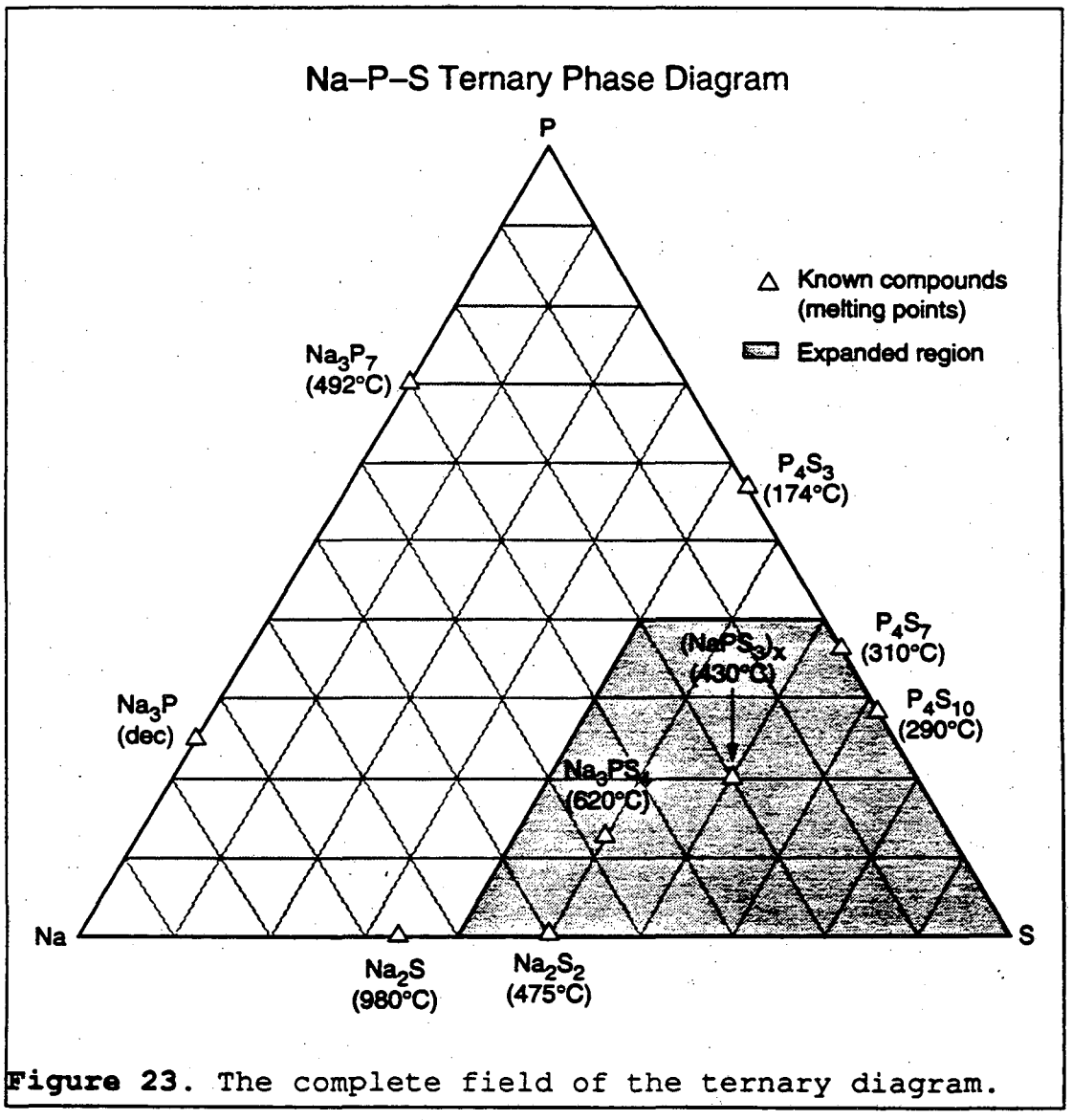

Figure 23. The complete field of the ternary diagram.

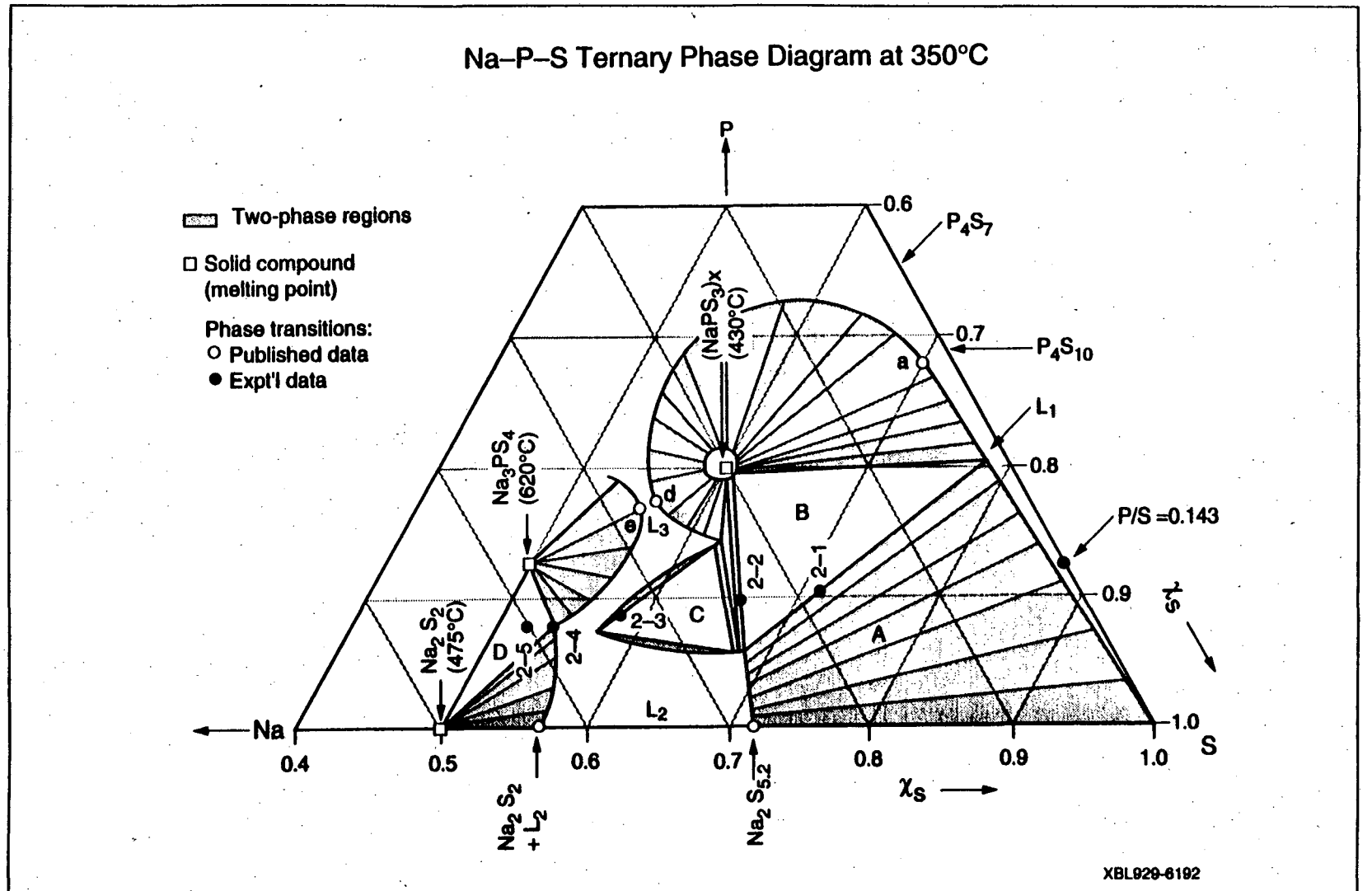

Figure 24. Proposed ternary diagram, 350 °C.

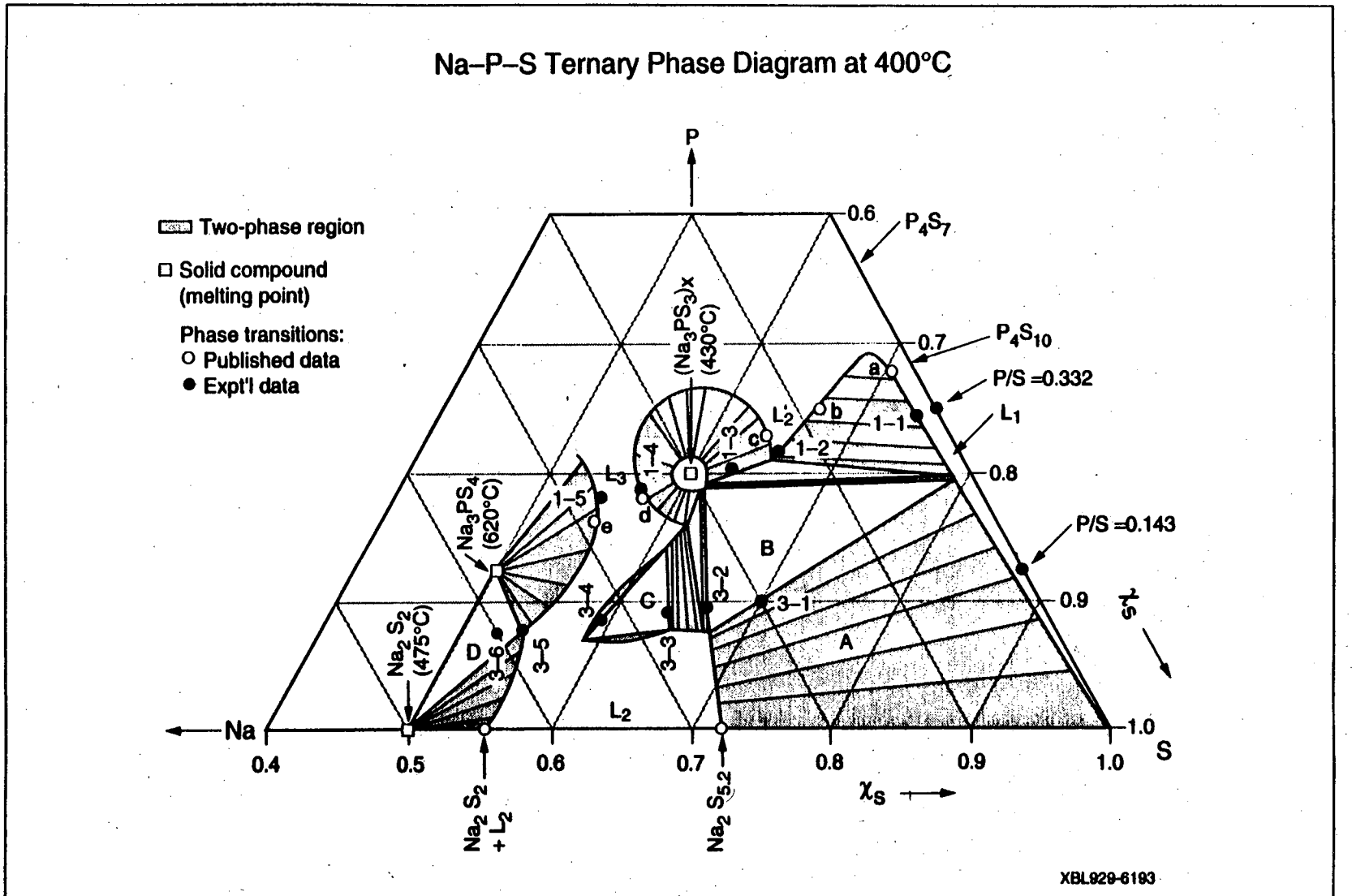

Figure 25. Proposed ternary diagram, 400 °C.

A solid (melting point 430°C), described as a ring-shaped polymeric compound of unknown size, formula $(NaPS_3)_x$[9], is represented in the Na_2S - P_4S_{10} phase diagram in Figure 3 and in Figure 24. In Figure 24 a proposed liquidus curve extending from a known phase boundary near the sulfur corner of the Na/S binary extends up parallel to the P-S binary without contacting it, which is consistent with the P-S phase diagram at 350°C[47]. Above the point where region B meets this curve, the curve marks the solubility limit of $(NaPS_3)_x$ in the liquid L_1. The curve must pass through points a and d, to be consistent with Figure 3.

The cell emf data for P/S = 0.143 at 350°C (Figure 15) have a gradually increasing slope between χ_{Na} = 0.0 and 0.13. This behavior is ascribed to the crossing of equilibrium tie-lines fanning out across the two-phase region A, shown in Figure 24. These tie-lines show how, for any given bulk composition within the boundaries of region A, the melt will partition between one of a small range of compositions of L_2, in equilibrium with one of a large range of compositions of L_1. As the cell is discharged, the bulk composition, as plotted in Figure 24, moves from the P-S axis towards the Na corner, along the path shown by the emf data for P/S = 0.143. Consideration of the path followed by the changing bulk electrode composition across the converging tie-lines shows

that as the cell is discharged through region A, the rate of change in composition of L_1, as a function of sodium mole fraction, increases. This may be related to the gradual increase in the slope of the emf curve (Figure 15) from χ_{Na} = 0.0 to 0.13. On the other hand, the slope in Figure 15 decreases between χ_{Na} 0.13 and 0.179. The change in cell emf is a function of the change in composition of L_2 as well as L_1 in this two-phase region, and the emf profile is the result of the changing sodium activities in both of these phases.

On charge, an emf plateau forms at 2.4 volts which extends to χ_{Na} = 0.238. Discharge data (points equilibrated after passage of current in the discharging direction) over the same composition range form a plateau at a considerably lower 2.32 volts.

The 2.4-volt plateau may be due to the formation of a meta-stable, non-equilibrium phase: This plateau has a fragile quality in that even very low discharge currents cause the cell emf to fall to, and equilibrate at, about 2.3 volts. The polarization data in Figure 21 show a charging curve that extrapolates to the 2.3-volt plateau at zero current, showing no sign of the 2.4-volt plateau at χ_{Na} = 0.20, which supports this hypothesis.

In any case, without more data the ternary diagram cannot distinguish one of these phases from the other, as they seem to be present over a single sodium composition range, χ_{Na} = 0.179 to 0.238. The zero slope of the emf profile in this region indicates the existence of the three-phase field B proposed in Figure 24. The placement of the corners of this field are tentative as only two data points (2-1 and 2-2) are directly related to the boundaries of this region.

A three-phase region such as B is the inevitable result of an interaction between region A and the liquidus region around $(NaPS_3)_x$. A bulk electrode composition within region B forms solid $(NaPS_3)_x$ and two liquids which form the endpoints of the tie line in region A which forms one boundary of region B.

The emf plateau between points 2-2 and 2-3 in Figure 15 strongly suggests a three-phase region C. Again, the paucity of data makes the placement of the corners of this region uncertain.

Thermodynamic consistency requires that a boundary of a three phase region be in contact with a single two-phase region, though that two-phase region may be extremely thin. Also, in a three-component system, when two two-phase fields come into contact, a three-phase field generally forms. Thus in proposing region C to be directly adjacent to region B,

construction of the diagram shows that there must be two distinct two-phase regions and a three-phase region between them. There is no evidence for these three phase-fields in the emf data at 350°C, presumably because they are very thin with respect to the resolution of the emf data. However, at least one two-phase region is quite evident between regions B and C at 400°C, as will be discussed below.

Though there is no experimental evidence for the existence of two-phase regions along the upper and lower boundaries of region C, there must be two-phase regions (perhaps very thin ones) at the interfaces between C and the single-phase regions L_2 and L_3, and they are shown in Figure 24.

The sloping region of the emf curve between 2-3 and 2-4 in Figure 15 denotes passage through a single-phase region which extends upwards from the known single-phase region along the Na/S axis. At 2-4, the flattening of the emf curve is probably due to entrance into a three-phase field D wherein the liquid has become saturated in Na_2S_2 and Na_3PS_4. Region D is the result of the interaction of the liquidus regions around Na_2S_2 and Na_3PS_4, and its existence could have been predicted without the emf data.

According to the Na_2S - P_4S_{10} phase diagram in Figure 3 the liquidus line marking the solubility limit of Na_3PS_4 must pass

through point e. In Figure 24 this line is extended down through point e until it connects to the liquidus line around Na_2S_2, which is drawn up from its known endpoint on the Na-S binary. Thus Figure 24 shows that liquid component of region D exists at the terminus of the junction of two two-phase fields, one of which precipitates Na_2S_2 and the other Na_3PS_4.

The Na_2S - P_4S_{10} phase diagram also indicates that all mixtures of Na_2S and Na_3PS_4 are solid up to over 400°C. The Na/S diagram (see Figure 2) shows that all mixtures of Na_2S and Na_2S_2 are solid below 475 °C. Thus it is also probable that all mixtures of Na_2S_2 and Na_3PS_4 are solid, which is a necessary condition for the existence of three-phase region D described above.

Given the proximity of point 2-5 to the high-melting compounds Na_3PS_4 and Na_2S_2 as shown in Figure 24, the drop in potential found at point 2-5 is probably due to insulation of the electrode due the combined effect of continuing formation of solid Na_3PS_4 and Na_2S_2.

The 400°C Ternary Phase Diagram

The ternary phase diagram at 400°C proposed in Figure 25 is similar to that for 350°C, with some important differences. The published binary Na_2S - P_4S_{10} phase diagram, Figure 3,

shows that above 350°C a new liquid phase L_2' appears as the liquidus curve around $(NaPS_3)_x$ shrinks away from contact with L_1. Phase L_2' coexists with L_1 in a new two-phase region between points a and b as shown in Figure 3 and in Figure 25. Phase L_2' becomes saturated with the solid compound $(NaPS_3)_x$ at point c as shown in the same two figures. As shown in the ternary diagrams proposed in Figure 24 and Figure 25, this is interpreted as the partial splitting of one two-phase region (L_1 + $(NaPS_3)_x$) at 350°C into two smaller two-phase regions (L_1 + L_2', and L_2' + $(NaPS_3)_x$) at 400°C. It is common that regions of immiscibility get smaller with increasing temperature.

The cell emf experiment with P/S = 0.332 was chosen to gather data which could be closely compared with the Na_2S - P_4S_{10} phase diagram. At 350°C, even at the beginning of discharge the cell equilibration time of several days was too long for practical experimentation. The long equilibration time implies the formation of solids at very low sodium concentrations, which is consistent with the creation of solid $(NaPS_3)_x$ at $\chi_{P_4S_{10}} < 0.89$ (equivalent to $\chi_S < 0.985$), as seen in the Na_2S - P_4S_{10} phase diagram just below 350°C.

At 400°C the rates of cell discharge and equilibration were much faster indicating liquid electrodes, which is consistent with the Na_2S - P_4S_{10} phase diagram above 350°C, at Na_2S

compositions up to point c. The first break in slope of the emf data, in Figure 17 at point 1-1, is consistent with the passage from the single-phase L_1 into the $L_1 + L_2'$ two-phase region as shown in Figure 25. This ternary plot also shows that point 1-1 aligns well with point a, which marks this same phase boundary in the $Na_2S - P_4S_{10}$ phase diagram in Figure 3. Point 1-2 in Figure 17 marks a decrease in slope which has been interpreted as passage from the $L_1 + L_2'$ two-phase region through a narrow section of the single-phase (L_2') region, and into the two-phase $L_2' + (NaPS_3)_x$ region as drawn in Figure 25. Inspection of the $Na_2S - P_4S_{10}$ phase diagram at points b and c shows the single-phase L_2' region to be much wider than it is near point 1-2, where the width of the single-phase region is apparently less than could be resolved by the emf data. This is interpreted in Figure 25 as the rapid convergence of the two two-phase regions. This convergence requires the formation of a three-phase region along the upper boundary of region B. Again, a thin two-phase region must be inferred to exist between this thin three-phase region and region B.

Further discharge of the P/S = 0.332 electrode was expected to show a break in the emf plot as χ_{Na} passed through 0.2, as the electrode composition at this point would be exactly that of the reported high-melting (430°C) compound $(NaPS_3)_x$, shown in Figure 3 as the vertical line at 33% P_4S_{10}[37]. However, the expected near-discontinuity in cell emf occurred at a sodium

mole-fraction of approximately 0.17 (point 1-3 in Figure 17 and in Figure 25). This composition translates to 40% P_4S_{10} in the Na_2S - P_4S_{10} phase diagram, in considerable disagreement with that published work. One explanation for this discrepancy may be that a kinetically rapid formation of a glassy (i.e. viscous and slow to equilibrate) product with sodium atom-fraction 0.17 occurred, and would have gradually decomposed to form a thermodynamically favored mixture of $(NaPS_3)_x$ and L_2, in agreement with the Na_2S - P_4S_{10} phase diagram.

Another possible explanation arises because during discharge, the sodium concentration at the electrolyte surface can be considerably higher than the bulk concentration. Thus, while the bulk χ_{Na} was 0.17, the local sodium concentration may have reached 0.20 or higher at the electrolyte surface, forming a solid coating of $(NaPS_3)_x$, which being a viscous polymer may not have equilibrated (dissolved) in the bulk melt. Then, upon further discharge, if sodium entering at the electrolyte surface drove the local sodium concentration higher than χ_{Na} = 0.2, liquid L_3 may have formed, though the bulk sodium content was still less than 0.2. This liquid, in combination with solid $(NaPS_3)_x$ may not have equilibrated in a viscous electrode melt, but may have determined the potential at the electrolyte surface causing the cell potential to drop to the 2.4 volt plateau, whereas at equilibrium this plateau would

have formed as the overall sodium atom-fraction increased above 0.2.

The compound $(NaPS_3)_x$ is represented in the ternary diagrams as a small open area rather than a single point. This implies some variablity in composition of the solid caused by partial solubility of sodium, phosphorus, and sulfur in that solid. The approximately sigmoidal shape of the emf plot at point 1-3 is consistent with this hypothesis. A sharp break in emf would have implied a much lower solubility of the individual components in the solid, given that the cell discharge passes directly through the composition of $(NaPS_3)_x$.

The next break in slope in Figure 17 occurs at point 1-4 which corresponds closely to point d in the Na_2S - P_4S_{10} phase diagram and in Figure 25. As shown in Figure 3 point d is at the boundary between the two-phase $(NaPS_3)_x$ + L_3 region, and the single-phase L_3 region. The increase in slope at 1-4 is consistent with transition from a two-phase to a single-phase region. At point 1-5, the precipitous drop in potential seen in Figure 17 is shown in Figure 25 to be caused by entrance into the two-phase region around the solid Na_3PS4. Point e in Figure 25 shows where this liquidus curve intersects the Na_2S - P_4S_{10} phase diagram. The voltage drop indicated by point 1-5 may have occurred prematurely because of the formation of a non-equilibrium coating of Na_3PS_4. However, the discrepancy

between point e and point 1-5 is not large, and the true liquidus line may actually pass through both points.

The cell emf data for P/S = 0.143 at 400°C (Figure 16) are similar to the results at 350°C (Figure 15), with some noteworthy differences. At 350°C the two regions of zero slope in Figure 15 appear to directly abut each other, indicating two adjacent three-phase regions, namely regions B and C in Figure 24. As discussed earlier, thermodynamic considerations require two two-phase regions and a three-phase region to exist between regions B and C, but the 350°C data show no sign of them. At 400°C there is a finite (but steep) slope between the two voltage plateaus in Figure 16 indicating a two-phase region between points 3-2 and 3-3. Figure 25 shows this new region to be due to the retreat (comparing to Figure 24) of the right hand side of region C away from the three-phase region B, which is essentially unchanged between 350 and 400°C.

At point 3-4 in Figure 16 the sharp increase in slope is due to transition to a single-phase region, as shown in Figure 25. Note that there is no sign in the emf data between points 3-4 and 3-5 of a transition through the (presumably thin) two-phase field which must exist along the lower border of region C. Point 3-5 marks a decrease in slope which could also be an ill-resolved, narrow emf plateau of zero slope. Point 3-6

marks a steep drop in emf, followed by a levelling off and long equilibration times.

Whether point 3-5 marks an emf plateau or merely a decrease in slope, the interpretation is nearly the same. If point 3-5 signifies a plateau, the electrode composition has entered the three-phase region D formed by intersection of the liquidus regions around Na_2S_2 and Na_3PS_4 as shown in Figure 25. This is the same interpretation as that given for the 350°C data points 2-4 and 2-5, in Figure 24. If point 3-5 marks a decrease in slope, the left-hand corner of region D has probably moved either up or down (compared to its position at 350°C), resulting in a cell discharge path through one of the two two-phase liquidus regions surrounding Na_2S_2 or Na_3PS_4. The electrode composition then enters region D at point 3-6, where the precipitation of Na_2S_2 and Na_3PS_4 cause the drop in cell emf and long equilibration times. This behavior is similar to that in the experiment at 350°C at point 2-5, and it is explained similarly, by passage into a three-phase region D where solid Na_3PS_4, solid Na_2S_2, and liquid L_2 are in equilibrium.

Phase equilibria - Conclusions

In Figure 24 and Figure 25, a tentative and qualitative picture of the phase equilibria of the sulfur-rich portion of

the Na-P-S system is proposed based on the emf data collected in this research, and on the available published information. The phase equilibria are complex in that there are probably at least three three-phase regions in the range of compositions studied. Many more data points are needed to clearly establish the phase equilibria of this portion of the Na-P-S system. In planning future experiments, these proposed ternary diagrams could be used to choose P/S ratios which would allow cell discharges through regions which would provide the most information for determination of the phase equilibria of the Na-P-S system.

Conclusions

Apparatus has been constructed for the measurement of equilibrium cell potentials of sodium-phosphorus-sulfur mixtures versus sodium at 350 to at least 400°C. This has been verified by reproduction of the well-known behavior of sodium/sulfur cells at these temperatures. Collection of equilibrium data for a sodium/phosphorus-sulfur cell over a single discharge/charge cycle required approximately two weeks of continuous operation.

Phosphorus-sulfur ratios of 0.143, 0.332, and 1.17 were investigated. The best cell performance was obtained with a P/S composition ratio of 0.143 in the positive electrode. This composition gave higher cell voltages versus sodium than the sulfur electrode, leading to a calculated theoretical specific energy 11 percent higher than that of the sodium/sulfur cell. Polarization measurements showed the phosphorus additive to degrade cell performance under the restricted conditions of those experiments.

The equilibrium cell emf data from experiments using P/S ratios of 0.143 and 0.332, along with published data, were used to infer some aspects of the phase equilibria of the Na-P-S ternary system at 350 and 400°C. The studied region was the sulfur-rich corner of the ternary diagram extending to a

sodium mole-fraction of 0.4 and a phosphorus mole-fraction of 0.25. At least three three-phase regions appear to exist. Phase diagrams have been proposed which are consistent with the experimental and published data. These diagrams could be used in the design of experiments for further clarification of the phase equilibria of this little-studied system.

References

1. Reprinted from Cairns, E. and Shimotake, H. Science 164, 1969, p.1347-1355.

2. J. L. Sudworth & A. R. Tilley, The Sodium Sulfur Battery, Chapman and Hall, Ltd. London, 1985, p. xi.

3. Cairns E. J., Steunenberg R. K., "High-Temperature Batteries", in Progress in High Temperature Physics and Chemistry, Rouse C. A. (ed.), vol. 5, Pergamon Press, N.Y., N.Y. 1973, p.83-5.

4. Of course this process must come to an end sometime, and when the sodium concentration gets high enough, Na_2S_2 solid forms, has no significant ionic conductivity, and significantly reduces the cell performance.

5. Sudworth and Tilley, p.6.

6. Ragnar Tischer, Ed., The Sulfur Electrode, Academic Press, N.Y., N.Y., 1983, p.68.

7. Sudworth and Tilley, p.145.

8. Op. Cit. p.282.

9. Blachnik, Rabe, Z. anorg allg. Chem. 462, 1980, p.199-206.

10. K. Moedritzer and J.R. Van Wazer, J. Inorg. Nucl. Chem., 25, 1963, p.683-690, 1963.

11. M. Ribes, B.Barran, J.L. Soquet, Journal of Non-Crystalline Solids, 38 & 39, 1980, p.271-276.

12. V.A. Maroni, Argonne Nat'l Lab Report ANL-7675 April 1970, p.146.

13. M.1. Kyle, H. Shimotake, R. Rubishko, F.J. Martino, Argonne Nat'l Lab Report ANL7775, April 1971, p.142.

14. Dri-Lab Model DLX-002-D-P Glove Box equipped with Model M040-2 Dri-Train for oxygen and moisture removal, Vacuum Atmospheres Corporation, Inc. Hawthorne, California

15. Model FA31110SA Trace Oxygen Analyzer, Delta F Corp., Woburn, Mass and System 580 Hygrometer, Panametrics Inc., Waltham, Massachusetts

16. Na, 99.99%, Lot# 45690, Noah Chemical, Farmingdale, New York

17. S, 99.9995%, lot# 25176, Noah Chemical, Inc.

18. Na_2S, 99.9%, lot# 19962-C-2, Cerac Inc., Milwaukee, Wisconsin

19. Na_3P, 99%, Lot# 22037-B-1-5, Cerac Inc.

20. P_4S_{10}, 99%, Lot# 003300TP, Aldrich, Inc., Milwaukee, Wisconsin

21. P_4S_3, tech., Strem Inc., Newburyport, Massachusetts

22. GP-3185 Vulcan XC72R, Fiber Materials, Inc. (Graphite from Cabot Corp, H.T.1 hr @ 2500C)

23. Betalyte BT-10, Ceramatek Inc. Salt Lake City, Utah.

24. Sudworth and Tilley, p.40,41.

25. Sudworth and Tilley, p19, 79.

26. Ceramatek, Inc.

27. Part # 614U5X-0012-2, Pressure Science, Inc., Beltsville, Maryland

28. Part # 50750-A-040-X, Key Bellevilles, Inc., Leechburg, Pennsylvania The 3/4 inch outside diameters of these disk springs was machined down to 5/8 inch to fit the established cell design.

29. aluminum foil, 0.254 mm thick, 99.5+ % pure, Alpha Ventron, Inc., Ward Hill, Massachusetts

30. "Graphite Spray" # 605, McKay Chemical Co., Los Angeles, California

31. The other possible leak is from one cell compartment to the other through the header/electrolyte-tube joint, or a crack in the electrolyte tube. The former occurs due to faulty workmanship in tube-to-header glass bonding, or corrosion of the glass at high temperature (over 400 °C). The latter occurs for many reasons, including generation of excessive potential gradients across the electrolyte. None of our leak-prevention strategies in cell design could address these problems, which also plagued this work.

32. One of these was the control experiment using a pure sulfur positive electrode. The other experiment was for P/S ratio 1.17 in the positive electrode, which the emf data clearly showed not to be viable in an energy storage cell, so the polarization experiment was not done.

33. Model 2961 Test Furnace, Applied Test Systems Inc., Saxonburg, Pennsylvania

34. Model 61010, Research Inc., Minneapolis, Minnesota

35. Hokuto Denko Ltd. GPIB Potentiostat\Galvanostat HA-320G, Hokto Corp., San Dimas, California

36. Model 2240B Data-logger, Fluke, Inc., Fremont California

37. The computer was equipped with a Model MBC-488 IEEE Bus card from Keithley-Metrabyte Inc., Taunton, Massachusetts

38. Davies, A.J., Thesis, University of Southampton, 1973. Also, Sudworth and Tilley, p.429.

39. There were only three clear opportunities in the data to do this calculation of uncertainty in χ_{Na}, though there were many opportunities to estimate emf reproducibility. This is because the data were taken by establishing a chosen value of χ_{Na}, and then measuring emf as a dependent variable. Thus there are many data pairs with the same value of χ_{Na} and different emf values. There are no data pairs in the sloping regions of the emf plots which have the same (or sufficiently close) emf values and different χ_{Na} values. This is because it was not possible to "choose" an emf value and measure a resulting χ_{Na}. Thus it was necessary to interpolate data points at the same emf to get a $\Delta\chi_{Na}$. In only three cases was there enough data in the vicinity for a reliable interpolation.

40. Calculated from published data cited in 38.

41. Cairns and Steunenberg, p.85.

42. H.G. von Schnering and W. Hönle, Z. anorg. allg. Chem. 456, 1989, p.194-206.

43. Olego, D.J. Physical Review B. 31, 4, 1985, p.2230-2239.

44. Santandrea, C. Mensing, H.G. von Schnering, Thermochim. Acta, 117, 1987, p.261-270.

45. W. Wichelhaus, H.G. von Schnering Naturwissenschaften 60, 1973, p.104.

46. M. Baudler, D. Düster, K. Langerbeins, J. Germeshausen, Angew. Chem. 96, 4, 1984, p.309-310.

47. R. Förthman and A. Schneider, Zeit. Phys. Chem. Neue Folge, 49, 1966, p.22-37.

APPENDIX

Computer Programs

For collection of emf data, an executable program (i3eflk23.exe) was compiled using Microsoft QuickC from two source-code programs, i3eflk23.c and flkisr19.c. The many header files required for this compilation include i3eio2.h, flkio2.h, as well as standard header files supplied with QuickC.

A non-standard library file (Xignall.lib) and four related header files (envir.h, 8259.h, xignal.h, and alarm.h were obtained from Professor Auslander, Dept. of Mechanical Engineering. They are required to service an interrupt routine which is used to set flags indicating when its time to collect a data point from the data logger, or to instruct the galvanostat to turn off the current to the cell. This could be rewritten to eliminate the interrupt routine, using a repetitive polling of the dos clock instead, with much greater simplicity. These five files are required to compile the program as written, and so are included in the diskette "i3eflk23" described below, but are not listed in this appendix, as they are not required for understanding of the source code.

A "make-file" which can be created and read only from within the QuickC environment must include i3eflk23.c, flkisr19.c, and xignall.lib as "source files". A "medium" or "large" memory model must be selected, and "incremental compile" must be unselected within the compiler options, and "incremental link" must be unselected also. The i3eflk23.mak file exists only in binary form, and therefore cannot be listed intelligibly here, but is supplied on the diskette"i3eflk23".

i3eflk23.exe interacts with the Metrabyte MBC-488 ieee bus card, which is installed at address H300 (i.e. 300, hexadecimal). This address is set on the card, and early in i3eflk23.c. The ieee card requires two device drivers. They must be defined, like other devices, in the config.sys of the host computer. The device files, dv488pc.sys and viparse.sys are supplied by Metrabyte Corporation on a diskette kept with the manual for the card, which is kept in LBL bldg. 70, room 218.

The program interacts with the Fluke Datalogger (a fancy A/D converter) via the ieee bus, at address 4. It interacts with the Galvanostat via ieee bus address 5. Good luck.

Except for the programming that interacts directly with the ieee card and the datalogger (the external devices), the code can be run for debugging purposes on a computer which does not have these devices installed, by placing the define "FAKE" in the compilation options of the make-file. Then data input to the program will be simulated, for the purpose of testing the main program.

All the required code, except for the Microsoft Quickc application, are kept on the diskette entitled "i3eflk23", on file in the office of Professor Elton Cairns.

Header Files

```
/********FLKIO2.H*************10/7/91**********************/

#define TICKTIME 50.0F
#include <dos.h>
#define DEVNUM 4
int flg,flg0,flg1,flg2,flg3,flg4,flg6,flg7,flg8,flg9,flg10,
    flg11,flg12,flg13;
int flg14,npts,autoflag,startflag,startdata(void),
    stopdata(void),state;
int gstremote(void),steps,ctr2,dev;
void discharger(void),delay(long),prmsg(int,int,char*),
    calculator(void);
void GetError(void),eqtest(void),flkcmd(char*),
     gstcmd(char*),pgrm(void);
void fakegstcmd(char*),fakeflkcmd(char*), realgstcmd(char*),
     realflkcmd(char*);
void getdata(void),plotdata(void),curparam(void),
     autocoul(void);
void realdata(void), fakedata(void), opendv488real(void),
opendv488fake(void);
char ipol[6],fname[15],fname2[15],inkey,comline2[17];
double realcur,idisch,eqtref,realont,maxcur,mincur;
double emf,curr,mins,temp,press;
float ifrac, irange,vdlim[6],dlim,oldlim,ontime,
      vsetcoul[6],deltaxna[6];
float setcoul,coul1,smmoles,XNa1,XNa2,coul2,coul3;
unsigned int daye,hr,min,sec, interval;
unsigned long secs, alarmint1;
struct dosdate_t ddate;
FILE *DV488,*DATA,*SUMDATA;
```

```
/***i3eio2.h***********10/4/91*********************
*** This is for use in the both computers******/
#ifdef FAKE
#define getdata() fakedata()
#define opendv488() opendv488fake()
#define gstcmd(char) fakegstcmd(char)
#define flkcmd(x)   fakeflkcmd(x)
#else
#define getdata() realdata()
#define opendv488() opendv488real()
#define gstcmd(char) realgstcmd(char)
#define flkcmd(x)   realflkcmd(x)
#endif
```

Main Source Code

```
/*************************************************************
*******************
*
*       I3EFLK23.C 12/11/91
*
*       IEEE-488 DEVICE DRIVER PROGRAM FOR FLUKE AND GALVAN
        OSTAT
*       It collects data from Fluke, and can automatically *
*       turn discharge current on and off.
*
*
*    Microsoft C V5.1
*
*   Serial Poll with String transfer
*
*************************************************************
******************/
#include <stdio.h>
#include <conio.h>
#include <stdlib.h>
#include <time.h>
#include <math.h>
#include "flkio2.h"
#include "i3eio2.h"
#include <string.h>
```

```
/*
*   This program assumes that the MBC-488 Board is at a base
address of 300 hex (768 dec).
*   To run with a different device number or base address,
*   change the following two lines.
*/


/*
*    Function Prototypes
*/
static char dciarg[2],chestarg[10];
static char basadr[] = "&H300";

void cls(void);


main(void)
{
    int itime,s=0;
    char comline[15];
    static int state=0;


    /* Get current date. */
    _dos_getdate( &ddate );

    flg0=0;

    smmoles=18.27F; /****P & S reset this for next
experiment!********/

    strcpy(fname,"DATA");    /* default output data file
name */
    strcpy(fname2,"SUMDATA");    /* default data summary
file name */

                        /** more default settings for Auto
Discharge **/
     idisch = -1.0;        /***default discharge current
(mA)***/
     dlim = 1.0F;             /**   millivolts/hr    **/
     npts = 14;
     maxcur = 5;                      /**  milliamps
**/
     mincur = .05;

    #ifdef FAKE
    interval = 1;
    emf = 2.7;
    #endif
```

```
    opendv488();

    fprintf (DV488,"BUFFERCLEAR\n");

    fflush(DV488);

    cls();

    prmsg (10,15,"Welcome to the automatic PxSy cell
discharger & data taker!");
    prmsg (20,15,"Enter current state of discharge
(coulombs):");
     scanf("%f",&coul1);
     coul2 = coul1;
    prmsg(22,15,"Current discharge state: ");
     printf("%.3f coul.",coul1);
/**    prmsg (24,15,"Enter millimoles of Sulfur Charged:");
     scanf("%lf",&smmoles);
      prmsg(26,15,"S charge:");
     printf("%.3g mmoles",smmoles);
 **/   printf("\n Caution: have you set overvoltage limits
and P/S charge?\n");
       printf("Have you removed any run-specific
instructions not intended here?\n");
     delay((long)2);
     XNa1 =(coul1/96.485) /(smmoles + (coul1/96.485));
     XNa2 =(coul2/96.485) /(smmoles + (coul2/96.485));

/*
*   Initialize the MBC-488 Board using the "SYSCON" command
*/

    fprintf (DV488,"SYSCON MAD1=3 CIC1=1 BA1=%s
CLK=4\n",basadr);

    if (fflush(DV488) == EOF)
    {
     GetError();
     return(0);
    }


/*
*   Set FLK to REMOTE, set default INTERVAL
*/
    flkcmd("E0");
    flkcmd("E1");
    flkcmd("I00,00,10"); /*Default  setting*/
    flkcmd("W2"); /***external interval data enable****/
/*
*   Set TIMEOUT (timeout time = 0.056 * itime)
*/
```

```
    itime = 100;
    fprintf (DV488,"TIMEOUT %d\n",itime);


    a1:
     cls();

    while(!kbhit())
     {
     switch (autoflag)
      {
       case 0:
     prmsg(6,11,"To toggle or see params of
AutoDischarge(OFF),type A");
     break;
       case 1:
     prmsg(6,11,"To toggle or see params of AutoDischarge
(ON),type A");
     break;
       case 2:
     prmsg(4,11,"Auto Discharging Stopped Due to Low or high
EMF!");
     prmsg(6,11,"To enable Automatic Discharge Operation
(OFF),type A");
     break;
      }
     if(state)
      {
       prmsg(3,11,"DATA IS BEING COLLECTED. To STOP,
   type S");
      }
     if (!flg4)
      {
       prmsg(11,11,"To continue gathering data (append)
    type C");
       prmsg(12,11,"To start gathering data, (write over)
    type D");
      }
     if (flg4 && !state) /**data files open, data not being
collected**/
      {
       prmsg(11,11,"To resume data collection,
    type D");
      }
     prmsg(9,11,"To issue a Fluke programming command,
 type P");
     prmsg(7,11,"To set/change Auto Discharge parameters,
 type O");
     prmsg(10,11,"To change mincur,
  type M");
```

```
     prmsg(8,11,"To change maxcur,
 type N");
     prmsg(13,11,"To exit program,
  type E\n\n\n");


      if (flg0)getdata();
      if (flg1)discharger();
      if (flg11)calculator();
     }

      inkey = (char) toupper(getche());        /* See if key
hit */

      switch(inkey)
     {
      case 'A':
     cls();
     if(autoflag)
       {
        prmsg(15,1,"Do you want to turn off Auto
Discharger(Y/N)?");
        inkey = (char)toupper(getche());        /* See if
key hit */
        if(inkey=='Y')
         {
          if (startflag) discharger();
          autoflag = 0;
          break;
         }
       }
     cls();
     prmsg(2,1,"");

     if(autoflag)
        printf("Presently executing step %d of
%d\n",flg13,steps);

     prmsg(4,1,"");
     if(flg14) printf("Working in mole fraction
increments\n");
     else printf("Working in coulombic increments\n");
     printf("initial current: %lf mA\n",idisch);
     for(s=1;s<= steps;s++)
      {
       if(ipol[s]=='+')printf("STEP %d is: charge\n",s);
       else printf("STEP %d is:discharge\n",s);
       if(!flg14)printf("setcoul%d: %.4f
coulombs\n",s,vsetcoul[s]);
       else printf("XNa increment%d: %.4g
\n",s,deltaxna[s]);
       printf("dlim%d: %.3lg mV/hr\n\n",s,vdlim[s]);
```

```
      }

/**     printf("\nCURRENT ON command to GSTAT:\n %s
%s\n","GST", comline2);**/
     printf("At this moment,idisch: %.4f mA dlim: %.3lg
mV/hr setcoul: %.2f coul\n\n",idisch,dlim,setcoul);


     printf("Hit a key when ready");
     inkey = (char) toupper(getche());        /* See if key
hit */
     cls();

     if(!autoflag)
      {
       printf("Do you want to start Autodischarge?(Y/N)\n");
       inkey = (char) toupper(getche());        /* See if
key hit */
       if(inkey == 'Y')
        {
         gstremote();
         if(state) flkcmd("S2"); /**if data was being
collected, need to **/
         autoflag = 1;  /**restart Fluke after sending a
command to gstat**/
         printf("\nAutomatic Discharge Mode will now begin
with Data Collection.\n");
         if(!state) delay((long)1);
        }
      }

     break;


      case 'G':
/**     plotdata();     **/
     break;

      case 'P':
     cls();
     prmsg(17,1,"Do you want to load default parameters ?
(Y/N)\n");


     inkey = (char) toupper(getche());        /* See if key
hit */

     if (inkey == 'Y')   /*load default parameters*/
          {
          prmsg(18,1,"Loading default parameters.../n");
          flkcmd("S0");
          flkcmd("W2");
```

```
            flkcmd("C020,4,00,00");
            flkcmd("C021,4,00,00");
            flkcmd("C022,4,00,00");
            flkcmd("C023,7,00,00");
            flkcmd("F020");
            flkcmd("L023");
            flkcmd("I00,00,10");
            flkcmd("T000,00,00,00");
            flkcmd("G000");
            flkcmd("K000");
            flkcmd("J00,00");
            eqtref = 0.0;/* resets equilibration timer*/
            break;
           }

      cls();
      prmsg(17,1," Type command string now:");


      gets(comline);
      strupr(comline);
      flkcmd(comline);
      break;


       case 'O':
      if(startflag) break;

      cls();
      prmsg(10,1,"How many steps in program(1-5)?");
      scanf("%d",&steps);
      while(steps > 5 || steps < 1)
       {
        prmsg(13,1,"steps must be between 1 and 5. Try
again:");
        scanf("%d",&steps);
       }

     prmsg(13,1,"Progam in coulombic increments(0) or mole
fraction(1)?");
      scanf("%d",&flg14);

       cls();
       prmsg(4,1,"initial current (mA):");

       scanf("%lf",&idisch);
         if(fabs(idisch)<0.010)
           {
            printf("\nYou can't go under .010 mA! Try
again");
            scanf("%lf",&idisch);
           }
```

```
        if(fabs(idisch) > 200.0 )
         {
           printf("Cant go over 200 mA! Try again");
           scanf("%lf",&idisch);
         }


      for(s=1;s <= steps;s++)
      {
       cls();
       printf("FOR STEP %d:\n",s);
       printf("current polarity(+ or -,for
charge/discharge):");
       do
        {
         scanf("%ls",&ipol[s]);
         if(ipol[s] != '-' && ipol[s] != '+')
           printf("\n You must enter + or - for polarity.
Try again:");
         }
       while(ipol[s] != '-' && ipol[s] != '+');
       if(!flg14)
        {
         printf("setcoul%d:",s);
         scanf("%f",&vsetcoul[s]);
        }
       else
        {
         printf("XNa increment%d:",s);
         scanf("%f",&deltaxna[s]);
        }
         printf("dlim%d (mV/hr):",s);
         scanf("%g",&vdlim[s]);

      }

      cls();
      prmsg(4,1,"");
      printf("initial current: %lf mA\n",idisch);
      for(s=1;s<= steps;s++)
      {
       printf("\ncurrent polarity %d: %c ",s,ipol[s]);
       if(ipol[s]=='+')printf("(charge)\n");
       else printf("(discharge)\n");
       if(!flg14) printf("setcoul%d: %.4f
coul\n",s,vsetcoul[s]);
       else printf("XNa increment%d: %.4g \n",s,deltaxna[s]);
       printf("dlim%d: %.3lg mV/hr\n",s,vdlim[s]);
      }
         flg13=1;
         pgrm();
```

```
        printf("Correct? and, ya wanna starterup?(Y/N)\n");

        inkey = (char) toupper(getche());        /* See if
key hit */

      if (inkey == 'Y')
       {
        if(!autoflag)
         {
          gstremote();
          if(state) flkcmd("S2"); /**if data was being
collected, need to **/
          autoflag = 1;  /**restart Fluke after sending a
command to gstat**/
         }
        else
        {
         ctr2 = 0;
         break;
        }
       }
      else autoflag = 0;


     ctr2 =  0;

     break;

      case 'M':
     cls();
     prmsg(15,1,"Presently, mincur is:");
     printf(" %.2lf",mincur);
     prmsg(17,1,"Do you want to change it?");

     if(toupper(getche())== 'Y')
      {
       prmsg(18,1,"Ok, new mincur is:");
       scanf("%lf",&mincur);
       printf("\n\nMincur is now %.2lf\n",mincur);
       inkey = (char) toupper(getche()); /*** hold till key
hit***/
      }

     break;

      case 'N':
     cls();
     prmsg(17,1,"old maxcur was");
     printf(" %.1lf mA\n",maxcur);
     prmsg(18,1,"New maxcur is (in mA):");
```

```
      scanf("%lf",&maxcur);
      printf("\nmaxcur is now %.1lf mA.",maxcur);
      if(!state) delay((long)2);
      break;

       case 'D':
      if(!flg4)
       {
        cls();
        printf("You wanna write over %s and %s if they
already exist?(y/n)\n",fname,fname2);
       if(toupper(getche())!= 'Y') break;
       }
     if (flg4==0)    /* open files and zero timer on first
entry into getdata()*/
       {

            if ((DATA = fopen (fname,"w")) == NULL)
             {
           printf("%c\nCould not open file %s.\n",fname);
           exit(0);
             }
            if ((SUMDATA = fopen (fname2,"w")) == NULL)
             {
            printf("%c\nCould not open file %s.\n",fname2);
            exit(0);
             }
           fprintf(DATA, "Date: %u/%02u/%02u \n",
              ddate.month, ddate.day, ddate.year - 1900);
           fprintf(SUMDATA, "SDate: %u/%02u/%02u \n",
              ddate.month, ddate.day, ddate.year - 1900);

            flg4 = 1;

       }
     if (!flg8) flg10 = 1;/***signals first entry into
startdata,
                     causing reset of eqtref when time is
read in****/
     state = startdata();

     break;

      case 'C':
      if(!flg4)
       {
     if ((DATA = fopen (fname,"a")) == NULL)
      {
        printf("\nCould not open file %s.\n",fname);
        exit(0);
      }
     if ((SUMDATA = fopen (fname2,"a")) == NULL)
```

```
        {
          printf("\nCould not open file %s.\n",fname2);
          exit(0);
        }
            fprintf( DATA,"File opened. \n");
            fprintf(SUMDATA,"File opened.\n");
           fprintf(DATA, "File opened. Date: %u/%02u/%02u
\n",
              ddate.month, ddate.day, ddate.year - 1900);
           fprintf(SUMDATA, "File opened. Date: %u/%02u/%02u
\n",
              ddate.month, ddate.day, ddate.year - 1900);

         }
      flg4 = 1; /**protection to avoid opening open files**/
      if(!flg8) flg10 = 1;/***signals first entry into
startdata, causing
                     ***reset of eqtref when time is read in.
Could enter
                     ***an eqtref manually here****/

      state = startdata();
      break;

       case 'S':
      state = stopdata();
      break;

       case 'E':
      if(state) state = stopdata();
      flkcmd("S0");
      flkcmd("E0");
      if(DATA != 0) fprintf(DATA,"program ended\n");
      fprintf(SUMDATA,"program ended at %.11f mins SOC=
%7.3f, last curr %.2f mA for %.11f
min\n",mins,coul1,realcur,realont);
      if(DATA != 0) fclose(DATA);
      fclose(DV488);
      if (SUMDATA != 0) fclose(SUMDATA);
      return(0);

      }
       goto a1;



}

/*************************************************************
**********
* Function to  Set GALVANOSTAT to REMOTE
```

```
*****************************************************************
*********/

int gstremote(void)
 {
     fprintf(DV488,"REMOTE %2d\n",5);

     if (fflush(DV488) == EOF)
      {
       GetError();
       return(0);
      }

 }
/*****************************************************************
*
*     Functions to output commands
*
*****************************************************************
*/

void realflkcmd(char cmd[50])
 {
      int hr=0,min=0,secs=0;


      if(sscanf(cmd,"I%2d,%2d,%2d",&hr,&min,&secs)==3)
        interval = 3600*hr + 60*min + secs;


       fprintf (DV488,"OUTPUT %2d $ ! %s\n",4,cmd);

       if (fflush(DV488) == EOF) GetError();

 }

void realgstcmd(char cmd[])
 {

      fprintf (DV488,"OUTPUT %2d $ ! %s\n",5,cmd);

      if (fflush(DV488) == EOF)
     {
       GetError();
       return;
     }
 }


/*****************************************************************
*
```

```
*
*       Function to print string to screen at coordinate
*       Uses ANSI.SYS
*
*************************************************************
/

void prmsg(int irow,int icol,char string[])
{
   char ESC = '\x1b';
   printf
("%c[%.*d;%.*dH%s",ESC,(int)(log10((double)irow))+1,irow,

(int)(log10((double)icol))+1,icol,string);
   return;
}

/*************************************************************
*
*    FUNCTION TO CLEAR SCREEN
*
*************************************************************
/

void cls(void)
{
  char esc = '\x1b';
  printf("%c[2J",esc);
  return;
}
/*************************************************************
*
*
*       Procedure to generate delay
*
*************************************************************
/

void delay(long numsec)
{
    long ltime,ntime;
    time(&ltime);
    while ((time(&ntime)-ltime) < numsec);

    return;
}

/*************************************************************
*
*
*       Procedure to Read and Print Error Strings from
Driver
```

```
*
**************************************************************
/

void GetError(void)
{
    char ErrorNum[20],OrigCommand[128],ErrorExplain[128];

    rewind(DV488);      /* Rewind Puts Device into Input Mode
       */

/* Use fgets, not fscanf because fgets uses carriage
return-line feed */
/* as delimiters between strings, fscanf uses blanks
       */
/* Get The Three Diagnostic Messages Here And Print Them Out
       */

    if (fgets(ErrorNum,10,DV488)   == NULL) exit(77);
    if (fgets(OrigCommand,128,DV488) == NULL) exit(78);
    if (fgets(ErrorExplain,128,DV488) == NULL) exit(79);

    cls();

    prmsg(14,6,"Error Number => ");
    printf ("%s\n",ErrorNum);

    prmsg(15,6,"Original Command => ");
    printf ("%s\n",OrigCommand);

    prmsg(16,6,"Error Description => ");
    printf ("%s\n",ErrorExplain);

    rewind(DV488) ;     /* Rewind Puts Device Back Into
Output Mode */
}

 void curparam()
  {
     double  estarg;

     if(fabs(idisch)<=0.020 && fabs(idisch) >= .010)
      {
       itoa(2,dciarg,10);
       estarg = idisch/.020;
       gcvt(estarg,4,chestarg);
      }
     if(fabs(idisch)<=0.20 && fabs(idisch) > 0.020)
      {
       itoa(3,dciarg,10);
       estarg = idisch/0.20;
       gcvt(estarg,4,chestarg);
```

```
        }
      if(fabs(idisch)<=2.0 && fabs(idisch) > 0.20)
        {
         itoa(4,dciarg,10);
         estarg = idisch/2.0;
         gcvt(estarg,4,chestarg);
        }
      if(fabs(idisch) <= 20.0 && fabs(idisch) > 2.0)
        {
         itoa(5,dciarg,10);
         estarg = idisch/20.0;
         gcvt(estarg,4,chestarg);
        }
      if(fabs(idisch)<=200.0 && fabs(idisch) > 20.0)
        {
         itoa(6,dciarg,10);
         estarg = idisch/200.0;
         gcvt(estarg,4,chestarg);
        }
      strcpy(comline2,"DCI");
      strcat(comline2,dciarg);
      strcat(comline2," IT1 EST");
      strcat(comline2,chestarg);
   }

/*
*   Open the device driver
*/
void opendv488real(void)
 {
    if ((DV488 = fopen ("$DV488","r+")) == NULL)
     {
        printf("%c\nCould not open device $DV488\n");
        exit(0);
     }
 }

void opendv488fake(void)
{
     if ((DV488 = fopen ("DV488","w")) == NULL)
      {
       printf("%c\nCould not open file DV488.\n");
       exit(0);
      }
}

void pgrm(void)
{
 float nxxna;
 if(ipol[flg13] == '+')
  {
   idisch = fabs(idisch);
```

```
    deltaxna[flg13] = -deltaxna[flg13];
   }
  if(ipol[flg13] == '-') idisch = -fabs(idisch);
  curparam();
  if(!flg14) setcoul = vsetcoul[flg13];
  else
   {
    nxxna = XNa1 + deltaxna[flg13];
    setcoul = (float)fabs(coul1 +
nxxna*smmoles*96.485F/(nxxna - 1.0F));
   }
  dlim = vdlim[flg13];
  oldlim = dlim;
  ontime = setcoul*16.67F/fabs((float)idisch);
  alarmint1 = (unsigned long)(ontime*60000.F/TICKTIME +
0.5F);
  if(!dlim) npts = 0;
  else npts = 14;
}




/*****************************FLKISR19.c 12-91******
for use with i3eflk23
******/

#include <stdio.h>
#include <conio.h>
#include "envir.h"
#include "8259.h"
#include "xignal.h"
#include "alarm.h"
#include "flkio2.h"
#include "i3eio2.h"
#include <math.h>
#include <stdlib.h>

static int flg5,ctr3,ctr5;
static unsigned long thyme1,alarmint0;
static float deriv, emfref;
static double curtmr,coultmr,eqtime;

/*******************************************************
*  Function to disable interrrupt, 'clean up workbench',
etc.
*******************************************************/

stopdata()
{
  if (startflag) discharger();
```

```
  autoflag = 0;  /***stops auto discharge**/
  setalarm(-1.0);
  xignal(XIGTMR,XIG_DFL);
  flg0 = 0;              /** turns off signal to collect
next data point**/
  flg8=1;  /***signal not to reset eqtimer on next
startdata()***/
  flkcmd("S0");
  fprintf(DATA,"data collection stopped. time %.2lf mins;
SOC: %7.3lf\n"
   ,mins,coul1);
  fprintf(SUMDATA,"data collection stopped.time %.2lf mins;
SOC: %7.3lf\n"
   ,mins,coul1);
  return(0);
}

/*********************************************************
* ISR to set flag for data collection
*********************************************************/

void flgup(void)
{
 static unsigned long int thyme0;
 int i;

     if(thyme0++>=alarmint0)
      {
       flg0 = 1;             /**indicates time to get
data**/
       thyme0 = 0;
      }
   #ifdef FAKE
     if(startflag && thyme1++>=alarmint1/10) flg1 = 1;
/***indicates time to
                                turn off discharge
current***/
   #else
     if(startflag && thyme1++>=alarmint1) flg1 = 1;
/***indicates time to
                                turn off discharge
current***/
   #endif

seoi(TMRVEC);
}

/*********************************************************
*  Function to assign isr routine, and enable the interrupt
*********************************************************/
```

```
startdata()
{
  #ifdef FAKE
  alarmint0 = (unsigned
long)(((float)interval)*1000.0F/TICKTIME + 0.5F);
  #else
  alarmint0 = (unsigned
long)(0.8F*((float)interval)*1000.0F/TICKTIME + 0.5F);
  #endif
  ctr5=0;
  flg5=1;         /**signal to reset minute timer for writing
data to file**/
  xignal(XIGTMR, flgup);
  setalarm(TICKTIME);
  flkcmd("S2");
  getdata();
  return(1);
}


/*************************************************************
*
*
*    function to collect real data. In other parts of this
program,
*    "getdata()" refers to "realdata()" or to "fakedata()"
depending on
*    whether the make file compile definition FAKE is being
used, which in
*    turn depends on whether the i3eflk__ .exe file is to be
used in a
*    computer which has an IEEE 488 card.
*
*************************************************************
/

void realdata(void)
{
     int i=0;
     long int req;
     char flk[81];
     static int ctr1;  /***ctr2 is defined in flkio2****/
     flg0 = 0;

 for(i=0;i<=3;i++)
  {
   do
    {
/*************************************************************
***************
*   Wait for SRQ
*/
```

```
        fprintf (DV488,"REQUEST\n");
        if (fflush(DV488) == EOF)
        {
          GetError();
          return;
        }
        rewind (DV488);

        if (fscanf (DV488,"%ld", &req) != 1)
        {
          printf("Fatal Error 1\n");
          /*   delay((long)1);   */
          return;
        }
        rewind (DV488);
       /*  printf ("ctr1= %d\r",ctr1);
      /*printf ("\nReq = %lx", req);*/

        if(ctr1++==20)
         {
      /*    printf("ctr1= %d\n",ctr1); **/
         if(flg5)
          {
           printf("missed1\n");
           fprintf(DATA,"missed1\n");
          }
         return;
         }
        if(ctr1>=26)
          {
           printf("Fluke isnt doing anything.\r");
          fprintf(DATA,"Fluke isnt doing anything.\n");
          flkcmd("S0");
          flkcmd("S2");
          flg0=1;
          flg5=1;
          ctr1 = 0;
          return;
          }
    }
   while ((req  & 0x4000) != 0x4000);  /* i.e. if no SRQ
sensed */



      ctr1 = 0;

/*
*  ********** Read data from FLUKE*******************/
```

```
    fprintf (DV488,"ENTER %2d  $\n",DEVNUM);  /* Ask for the
data */
    if (fflush(DV488) == EOF)
      {
       GetError();
       return;
      }
    rewind(DV488);


    if (fgets(flk,80,DV488) ==NULL)      /* Read the data
from the FLK */
      {
       printf("\nFatal Error\n");
       return;
      }
    rewind(DV488);

        /* Print the data

    fprintf(DATA,"raw: %s",flk);
    printf("raw: %s",flk);*/



  if(i == 0)
   {
     if(sscanf(flk,"Y%d:%d:%d:%d",&daye,&hr,&min,&sec) != 4)
       {
        if(ctr2>=6)
         {
          printf("missed for the last time. ctr2=
%d\n",ctr2);
          exit(0);
         }
        printf("\rMissed and going around again. Ctr2 =
%d",ctr2);
   /*      printf("\nRaw: %s",flk);     */
   /*      fprintf(DATA,"missed on: %s\n",flk);  **/
   /*      delay((long)2);    */
        ctr2++;
        flg0=1;
         if(flg5)
          {
           printf("missed2\n");
           fprintf(DATA,"missed2\n");
          }
        return;
       }
     ctr2=0;
    /** printf("sec= %d\n",sec);  */
   }
```

```
  if(i == 2)
   {
    if(sscanf(flk,"A 20 %lf %*4s A 21 %f V A 22 %f V A 23 +
%lf C",&emf,&ifrac,&irange,&temp)!=4)
       {
        i=0;
    /*     printf("stopdaglitch");       */
         if(flg5)
          {
           printf("missed3\n");
           fprintf(DATA,"missed3\n");
          }
        return;
       }
    mins = (double)(60*(hr + 24*daye) + min) +
((double)sec)/60;
    irange = (float)((int)(2.0F*irange + 0.5F));
    curr = ifrac*.002*pow(10,irange);

    /*****************curr and emf
calibrations***************************/

    if(curr < 0.0) curr = 0.99193*curr - .000277;
    else curr = 0.998660*curr - 0.001155;

    emf = 1.001155*emf -.000084;
    flg11=1;
   }
  }
 return;
}

/*************************************************************
**************
*** function to print data, decide when to discharge cell,
count coulombs,
*** guard against overvoltage, etc.
*************************************************************
**************/
void calculator(void)
 {
  int j=0;
  float newv, oldv,nxxna, soc3;
  static int flg2,tref,secdiff;
  static float voltarr[30];
  double telapsed1 = 0.0;

     flg11=0;

     telapsed1 = mins - curtmr;
```

```
      if (flg10)
       {
        eqtref= mins;
        flg10 = 0;
       }

      eqtime = mins - eqtref;
      temp = .99514*temp - .14840;

      /*  printf("%lf\t%f\n",mins,emf);     */
      for(j=(2*npts-2);j>=0;j--) voltarr[j+1] = voltarr[j];
      voltarr[0] = (float) emf;
      ctr3++;            /* number of array elements which
have been filled */
      if(ctr3>=(2*npts))    /* with valid info */
        {
         oldv=0.0F;
         newv=0.0F;
         for(j=0;j<=(npts-1);j++)
           {
            oldv += voltarr[j+npts];
            newv += voltarr[j];
           }

          if(npts) deriv = (newv -
oldv)*3.6e6/(interval*npts*npts);

           /***position cursor****/
           prmsg(16,1," ");
           printf("\remf: %.4lf V  DV:%7.2f mV/hr  Current:
%.4lf mA  Temp %5.1f C    \n\n",emf,deriv,curr,temp);
           printf(  "SOC1 : %7.2f Coul  XNa1: %8.3g  SOC2:
%7.2f Coul  XNa2: %8.3g \n\n",coul1,XNa1,coul2,XNa2);
           if(autoflag)
            {
             printf("Autodischarge on step %d of %d
\n\n",flg13,steps);
            }
           else printf("
    \n\n");

           if((fabs((double)deriv) <= dlim)||!dlim)
            {
             if(autoflag==1 && !startflag &&
(ctr5++>=12||!dlim))
               {                                    /**i.e. if
it is time to **/
                 ctr5=0;                             /**turn on
current**/
```

```
                if(!flg12)ontime =
setcoul*16.67F/fabs((float)idisch);

                if(flg12==1)ontime = (ontime - (float)
realont)/.75F;

                if(flg12==2)ontime = (ontime - (float)
realont)*.75F;

                alarmint1 = (unsigned
long)(ontime*60000.F/TICKTIME +0.5F);

                flg12 = 0;

                flg2 = 1; /**signal to write data, 1rst
interval after I on.*/

                discharger();

                return;
              }
            }
            else ctr5=0;

        }

      else
        {
         /***position cursor****/
         prmsg(16,1," ");
         printf("\remf: %.41f V  Dlim:% 5.1f mV/hr  Current:
%.41f mA  Temp %5.1f C    \n\n",emf,dlim,curr,temp);
         printf(  "SOC1: %7.2f Coul  XNa1: %8.3g  SOC2: %7.2f
Coul  XNa2: %8.3g \n\n",coul1,XNa1,coul2,XNa2);
        }
      if(startflag) printf("\rCurrent has been on %.11f out
of %.1f mins.      ",telapsed1, ontime);
      else printf("\rEquilibration time elapsed %.1f mins.
        ",eqtime);

      if(flg5)      /**tref and secdiff allow recording of
datapoints every**/
        {           /**minute, even after an interruption in
data taking**/
         tref=sec;
      /*   printf("tref=%d\n",tref);  */
         flg5=0;
        }

      secdiff = sec - tref;
```

```
     if(abs(secdiff)<=2 && !flg2 && !flg3)    /***Record
normal datapoint****/
       {
        fprintf(DATA,"%9.3lf min %6.4lf V %11.5lf mA %5.1f C
%3.1f mV/hr\n",mins,emf,curr,temp,deriv);
       }

    /*Record  datapoint if: 1) is at the end of the next
interval after
                          current was turned on (flg2), or
                       2) is at the end of the next interval
after
                          current was turned off (flg3).

    ************************/

     if(flg2)
      {
       curtmr = mins; /**gets time current was turned on**/
       coultmr = mins;/** ditto, for improved coulometer
autocoul()**/

       fprintf(DATA,"%9.3lf %6.4lf%11.5lf %5.1f I onned
now!\n",mins,emf,curr,temp);
       fprintf(DATA, "Date: %u/%02u/%02u \n",
             ddate.month, ddate.day, ddate.year - 1900);
       fprintf(SUMDATA, "SDate: %u/%02u/%02u \n",
             ddate.month, ddate.day, ddate.year - 1900);
       flg2 = 0;
      }

     if(startflag && !flg3) autocoul(); /**this is the
constantly updated
                       coulomb counter. the if conditions are
redundant.***/


     if(flg3)
      {
       coul1 -= telapsed1*realcur*.060;

       /**coul1 coulomb counter assumes the last current
reading was the true
       value the whole time the current was on. The results
of both coulomb
       counters (variables coul1 and coul2) are virtually
the same  **/

       realont = telapsed1;
       autocoul();
       eqtref = mins;
       XNa1 =(coul1/96.485)/(smmoles + (coul1/96.485));
```

```
        fprintf(DATA,"%9.3lf %6.4lf%11.5lf %5.1f SOC: %.3f
SOC2: %.3f I offed now!\n",mins,emf,curr,temp,coul1,coul2);

        if(!flg12)
         {
          if(++flg13<=steps) pgrm();
          else
           {
            dlim = vdlim[steps];
            if(flg14)
             {
           nxxna = XNa1 + deltaxna[steps];
           setcoul = (float) fabs(coul1 +
nxxna*smmoles*96.485/(nxxna - 1.0));
             }
           }
         }


/*********special instructions for use in a single
customized expt **********/


if(coul1 > 1000.0F)
 {
  idisch = fabs(idisch);
  curparam();
  maxcur = 10.0;
 }


/*************************************************************
*****************/
        flg3 = 0;

       }


      if(startflag && (fabs (emf - (double) emfref) >= 0.3))
       {
        discharger(); /* stops discharge if emf gets too
low/high */
        idisch = idisch*.75;
        if(fabs(idisch)> mincur)
         {
          flg12 = 1; /*** signal to reset ontime next time**/
                   /*** current is turned on
     **/
          dlim = 1.0e7F;
         }
        else
```

```
        {
         if(idisch > 0) autoflag = 0; /**turn off autodchg
at top of chg*/
         idisch = -1.333F*idisch; /***at bottom of dchg make
curr > mincur
                          and start charge****/
        }
       curparam();
      }

     if((startflag != 0) && (fabs (emf - (double) emfref) <=
0.05))
      {
       if(telapsed1 > 20.0 && fabs(idisch) < maxcur)
          /*don't want current over*/
          /*maxcur or to increase current too rapidly*/
        {
          flg12 = 2; /*** signal to reset ontime next
time**/
               /*** current is turned on
   **/
          discharger(); /* stops charge/discharge if low
overpotential*/
                 /* would allow current to be higher*/
          idisch = idisch * 1.333;
          dlim = 1000.0F;
          curparam();
        }
      }

/******enable this function for real cell!***********/

      if(startflag && emf<1.0)
       {
        autoflag = 0;
        discharger();
       }

/*****************************************************/

      if(!startflag && fabs((double)curr)>.010)
       {
        if(!autoflag)gstremote();
        startflag=1;    /*** extra precaution to turn off
current if**/
        discharger();      /*** a gstcmd is ignored***/
       }
```

```
/***instructions to stop on a specific voltage plateau**

      if(startflag && (XNa1 < .15 || coul2 > 1450))
       {
        autoflag = 0;
        discharger();
       }


**********************************************************
/
 }
/**********************************************************
******
* discharger function
**********************************************************
*******/
void discharger(void)
{
  if(startflag)              /*****turns current off when
'ontime'is reached*/
    {                        /***or due to too high/low
current***/
     startflag=0;
      fprintf(DATA,"%9.3lf %6.4lf%11.5lf %5.1f I
offing!\n",mins,emf,curr,temp);
     realcur = curr; /**realcur is printed in datafiles,
but also
                  used in last calc of autocoul, i.e. after
                  next data collection, where curr = 0, and
would
                  give an erroneous result.**/

     flg1 = 0;     /****flg1=1 indicated normal time to turn
off current***/
     thyme1=0;   /****counter for current time, now
rezeroed***/
     flg3 = 1;       /****signal to record next datapoint in
file***/
     gstcmd("IT0 DCI0 EM");
    }
   else
    {                    /**turns current on when dlim is
reached**/
     emfref = (float) emf;
     gstcmd("GST");
     gstcmd(comline2);
     fprintf(DATA,"%9.3lf %6.4lf %10.5lf %5.1f %8.3f Eeq,I
onning!\n",mins,emf,curr,temp,coul1);
     fprintf(SUMDATA,"%9.3lg %.4lf %8.3fcl %5.1fC %5.1fmeq
%4.2gmV/hr%5.3gmA %5.2lf
```

```
%.21fmon\n",XNa1,emf,coul1,temp,eqtime,dlim,idisch,mins,real
ont);
      startflag = 1; /****signal that current is on ***/
      npts =14; /**reenables derivative counter if offed for
dlim=0**/
    }
   flg5=1; /** signal to reset tref, and output error
messages if data missed**/
   flkcmd("S0");
   flkcmd("S2");
   getdata();
}

void autocoul(void)
 {
  double telapsed2 = 0.0;
  telapsed2 = mins - coultmr;
  /**see note on realcur in discharger()***/
  if(flg3) coul2 -= telapsed2*realcur*.060;
  else coul2 -= telapsed2*curr*.060;
  XNa2 =(coul2/96.485)/(smmoles + (coul2/96.485));
  coultmr = mins;
 }
void  fakedata(void)
 {
  static long int i;
  static long int j;
  static double a;
  flg0 = 0;
  if (startflag)
   {
    emf += idisch/(1000 + (double) 2000*j++);
    curr = idisch;
    i=0;
   }
  else
   {
    a =  (double) (5000*i++);
    curr = 0.0;
    emf -= idisch/(10000.0 + a);
    j = 0;
   }
  mins = mins + .167;

  flg11 =1;
 }

void fakegstcmd(char *cmd)
 {}

void fakeflkcmd(char *cmd)
{}
```

Emf Cell - Dimensions

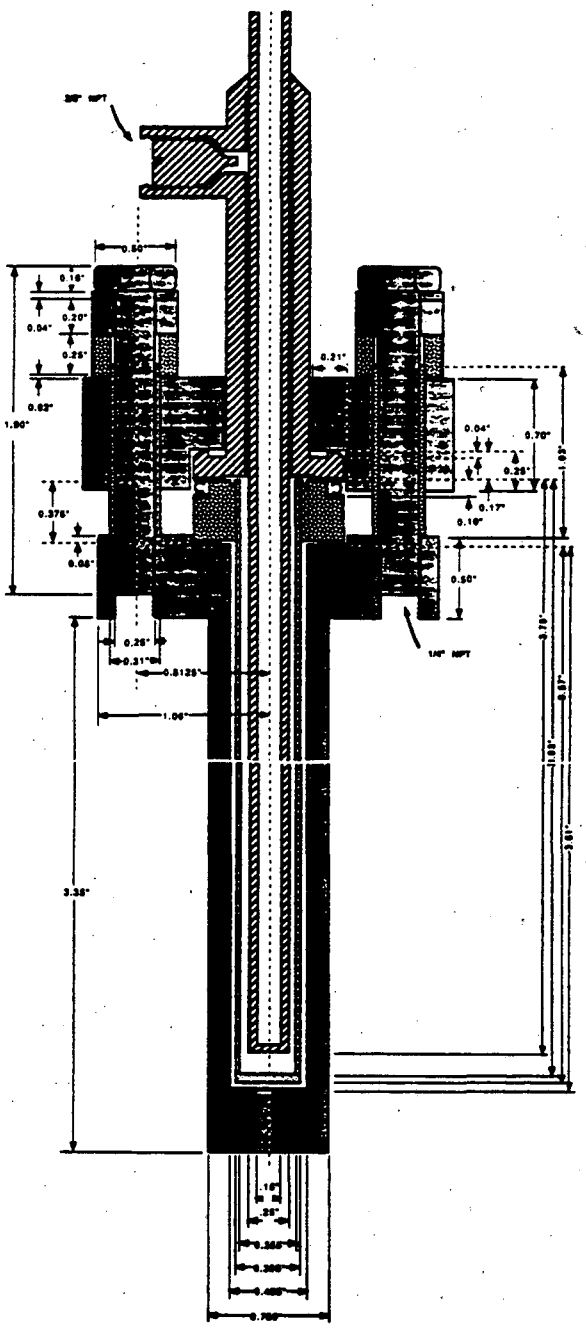

LAWRENCE BERKELEY LABORATORY
UNIVERSITY OF CALIFORNIA
TECHNICAL INFORMATION DEPARTMENT
BERKELEY, CALIFORNIA 94720